FURTHER DEVELOPMENT OF A PNEUMATICALLY POWERED MOTION SYSTEM FOR A HIGH-SPEED SCANNER

A Thesis
Presented to
The Academic Faculty

by

Matthew S. Boyd

In Partial Fulfillment
Of the Requirements for the Degree
Master of Science in the
George W. Woodruff School of Mechanical Engineering

Georgia Institute of Technology
April, 2004

FURTHER DEVELOPMENT OF A PNEUMATICALLY POWERED MOTION SYSTEM FOR A HIGH-SPEED SCANNER

Approved by:

Dr. Stephen L. Dickerson, Advisor

Dr. Steven Danyluk

Dr. Itzhak Green

Date Approved: April 12, 2004

ACKNOWLEDGEMENTS

I thank Brad Butcher for his excellent and extensive work on this project, without which my work would not have been possible. I thank Scott Coleman at CAMotion Inc. for always being willing to offer his help and advice on this project. I thank David Batcher and Misty Ellis at Southern Perfection Fabrication for manufacturing the weldment used in the vibration isolation system. I thank John Graham, Donald Long, and Thomas Newton in the machine shop for machining various other parts for this project. I thank Lizheng Zhang and William Limousin for their contributions and work on this project. Also, I thank Dr. Dickerson for his constant patience and instruction throughout the course of this project.

TABLE OF CONTENTS

LIST OF TABLES

LIST OF FIGURES

LIST OF SYMBOLS

At times in this paper, there are symbols being used to denote variables and symbols being used to denote units appearing in the same equation. To avoid confusion, this list is divided into symbols for variables and symbols for units.

VARIABLE SYMBOLS

A	cross-sectional area of the needle
a	acceleration of the scanner head caused by the force of the piston
B	damping constant
b	width of spring steel cross section
C	a constant
D	needle diameter
d	distance between the leading edges of each of the arms on the scanner head flag
d_c	the cylinder bore size
d_r	rod diameter
E	elastic modulus of spring steel
E_{Al}	elastic modulus of aluminum
e	roughness
F	force in the vibration isolation system model
F_f	force of piston friction
F_1	force exerted on the needle opening by the air in the tank

F_n force on the scanner head caused by the introduction of the air from the needle

F_p force exerted by the piston

f friction factor

f_R effective area on rid side of cylinder

f_p effective piston area

g acceleration due to gravity

h height of spring steel cross section

h_l major head loss

h_{lm} minor head loss

h_{lT} total head loss

I moment of inertia of cross section of spring steel strip

K minor loss coefficient

k spring constant

L needle length

L_e equivalent length in buckling equation

L_1 length of scanning path

L_f total energy lost to piston friction

L_m total energy lost to momentum transfer

L_s length of spring steel strip

M moment applied to air bushing

M_1 mass of scanner head in system model

M_2 mass of large, suspended mass in system model

m_1 mass of air in precharge volume before precharging begins

m_2 mass of air in precharge volume after precharging is complete

m_a mass of air in tank when the needle engages

m_n mass of air lost through the air bearings during one pass down the track

m_s mass of the scanner head

m_p combined mass of the rod and piston

$\dot{m}_a$ total mass flow rate out of the air bearings

$\dot{m}_n$ mass flow rate out of the needle

n a constant

P force that deflects a beam

P_1 pressure in supply tank in Section 2.1.1; pressure in precharge volume before precharging begins in Section 2.2.3

P_2 pressure at needle outlet in Section 2.1.1; pressure in precharge volume after precharging is complete in Section 2.2.3

P_a the minimum required pressure to ensure proper operation of the air bearings

P_c precharge pressure

P_n supply pressure to the needle

P_s supply pressure to the cylinder

Q volumetric flow rate

q_1 state 1 (position of scanner head) in state-space model

q_2 state 2 (position of suspended mass) in state-space model

q_3 state 3 (velocity of scanner head) in state-space model

q_4 state 4 (velocity of suspended mass) in state-space model

$\vec{q}$ state vector in state-space model

$\dot{\bar{q}}$	rate of change of state vector in state-space model
Re	Reynold's number
R_a	ideal gas constant for air
r_n	distance from center of gravity to the point where the needle engages
r_p	distance from center of gravity to the point where the piston force is applied
T	ambient temperature in which the scanner operates
T_1	period of the scanner head
t	time it takes the scanner head to make one pass down the track
t_a	time it takes to accelerate the scanner head to the desired velocity
t_c	time it takes to supply the required amount of air to the precharge volume
t_δ	the amount of time the needle is engaged with the tank
U	centerline velocity
V	volume of the tank on top of the scanner head
V_1	initial volume in isentropic expansion equation
V_2	final volume in isentropic expansion equation
V_{atm}	volume at which the pressure on the rod side reaches atmoshperic
V_c	precharge volume
v	average velocity
v_1	average velocity of air in supply tank
v_2	average velocity of air at needle outlet
v_{des}	desired velocity of the scanner head
W	work
x	lateral deflection in pendulum effect illustration

x_1 position of scanner head in vibration isolation system model

x_2 position of suspended mass in vibration isolation system model

$\dot{x}_1$ velocity of scanner head in vibration isolation system model

$\dot{x}_2$ velocity of suspended mass in vibration isolation system model

$\ddot{x}_1$ acceleration of scanner head in vibration isolation system model

$\ddot{x}_2$ acceleration of suspended mass in vibration isolation system model

z_1 elevation at state 1 (supply tank at 110 psig)

z_2 elevation at state 2 (needle outlet at 60 psig)

α displacement angle in pendulum effect illustration

Δ vertical displacement in pendulum effect illustration

δ deflection of a beam

δ_A total deflection of spring steel strip

δ_{atm} distance the piston must displace to get the rod side to reach atmospheric pressure

δ_{des} the distance required for the piston force to accelerate the scanner head to the desired velocity from rest

ξ damping ratio

μ dynamic viscosity of air

ρ_a density of air

ω_n natural frequency of suspended mass

UNIT SYMBOLS

cm centimeters

GPa	gigaPascals
in	inches
K	Kelvins
kg	kilograms
kPa	kiloPascals
m	meters
mm	millimeters
ms	milliseconds
N	Newtons
Pa	Pascals
psia	absolute pressure in pounds per square inch
psig	gage pressure in pounds per square inch
rad	radians
s	seconds

SUMMARY

This paper details the redesign of a previous pneumatic motion system for a linear scanner to meet higher performance requirements. The previous design featured a scanner head, two air bearings, and two pneumatic cylinders and was intended to propel the scanner head back and forth in a linear motion at speeds up to 5 m/s. Air was supplied to the air bearings by tethering the scanner head to an air supply with plastic tubing. At speeds nearing 5 m/s, the tether began to oscillate violently and the repeated impacts of the scanner head and pneumatic cylinders caused the entire structure to vibrate. Also, large amounts of energy were lost due to momentum transfer between the scanner head and cylinders and friction within the cylinders themselves. Further, none of the energy of the impact was recovered.

These problems were corrected by designing and purchasing new equipment and slightly altering the operation of the scanner. A system of needles was designed to provide air to the air bearings without the use of a tether. New pneumatic cylinders with exceptionally low friction were purchased and a method of precharging the air on the rod sides of the cylinders to a certain pressure was devised to add energy back into the system that is lost during operation. A special valve was designed to accomplish the addition of air into the precharge volumes. Also, a mechanism was designed to greatly minimize the vibration of the table. This structure consists of a large, suspended, inertial mass which holds the pneumatic cylinders so they are not actually mounted on the table which holds the scanning track.

CHAPTER 1

INTRODUCTION

1.1 The Previous Design

The purpose of the scanning motion system which is the subject of this paper is to aid in the surface imaging of circuit boards or other flat surfaces. As an example application, it is necessary to use some sort of surface imaging to inspect the solder paste layout on circuit boards before the various circuit elements are added. The image is created by moving a sensor over the entire area of the circuit board. This can be done in several ways, each involving a certain motion of the circuit boards and a certain scanning motion. The simplest method of doing this is to use a linear scanning motion. With this method, the scanner head moves over the top of the circuit board horizontally. When it reaches the end of the track, the circuit board is fed forward a certain increment and the scanner head moves back to the other end of the track making another pass across the board. By this process, the sensor can cover the entire area of the circuit board and create a surface image. Clearly the scanning speed determines the time required to produce and image of the surface.

Mr. Brad Butcher designed and built a preliminary version of the linear motion system described above. That design featured a scanner head that slid along a track through the use of two air bearings. One was a flat air bearing that glided over a smooth, flat metal surface and the other was an air bushing. These air bearings provided the scanner head with a nearly frictionless ride. The necessary air was provided to those bearings by tethering the scanner head to an air supply with a piece of plastic tubing. At

each end of the track was a small, pneumatic cylinder used to propel the scanner head in the opposite direction. The system was controlled by a model predictive control scheme using the Motorola MC68HC11E9 microcontroller. Two valves were used to connect and disconnect the cylinders to the pressure supply and two optical encoders were used to measure the velocity of the scanner head. Based on the measured scanner head velocity and the system parameters, the microcontroller calculated the necessary times to actuate each of the valves in order to get the scanner head to converge to the desired velocity in an appropriate amount of time. That design was unique in the fact that it used a system of fast-acting valves and pneumatic cylinders to move the scanner head instead of a linear motor. The successful operation of that motion system showed that Mr. Butcher's design was feasible and that it could be reasonably modified to meet certain higher performance requirements.

CHAPTER 2

NEW MOTION SYSTEM DESIGN

2.1 Tetherless Operation

One of the main objectives of this project was to design and implement a mode of tetherless operation of the scanner. In order to remove the tether, some other way had to be devised to provide the necessary air to the air bearings. The way that was finally chosen to accomplish this was to put an air-supply needle at each end of the track. In the previous design, a small tank was already mounted on top of the scanner head and used to provide air to the air bearings. A pressure supply was used to maintain the pressure in this tank at 60 psig. In the new design, two needles each supply the air necessary to keep the tank pressure greater than or equal to 60 psig. These needles engage with the scanner head after each pass down the track and are designed to supply at least the same amount of air that was expelled out of the air bearings during that pass. They are positioned so they engage with the tank for the same amount of time that the scanner head is in contact with the rod during the rebound.

Obviously, the amount of air expelled out of the air bearings during one pass is different depending on the velocity of the scanner head since the time it takes to make that pass varies with the velocity. However, the amount of time that the scanner head is in contact with the rod, and therefore the amount of time available to supply air to the tank, also varies with velocity. At slower velocities, more air is expelled since it takes the head longer to travel down the track, but the rebound process also takes longer which means that there is more time to replace that air. The opposite is true for higher

velocities. The travel time is shorter, but the available replacement time is shorter as well. Due to this fact, the desired velocity for which the greatest mass flow rate out of the needle would be required was not initially obvious. Therefore, in the analysis that follows it is initially left as a variable.

2.1.1 Design of Needles

In order to properly design the needles we must determine satisfactory dimensions that will make it possible to supply the tank on the scanner head with a sufficient amount of air to ensure proper operation of the air bearings. We will begin by assuming that a needle will be placed at each end of the track. Therefore, only the air lost during one pass down the track will need to be supplied by the needle. The first step is to determine the required mass flow rate out of the needles. Once this mass flow rate is known, we can calculate the necessary needle length and diameter by evaluating the head losses as will be shown.

The time that it takes for the scanner head to make one pass down the 46-cm track is

$$t = \frac{0.46m}{v_{des}} \qquad 1)$$

where v_{des} is the desired velocity. As described above, the desired velocity is an unknown for now, since it is not certain at which speed the largest mass flow rate from the needle will be required. We can model air as an ideal gas, so the ideal gas law will govern the mass of air in the tank at a given pressure. Assuming that the air bearings need at least 60 psig (414 kPa) to function properly, we will let P_a = 60 psig (or 74.7 psia

= 515.4 kPa) be the pressure in the tank at the time the scanner head hits the rod and the needle engages. The tank volume is 6.03 x 10^{-5} m^3, the room temperature is 293.15 K, and R_a is 0.2870 (kPa·m^3)/(kg·K) for air.

Therefore, the mass of air in the tank when the needle engages is given by the following equation.

$$m_a = \frac{P_a V}{R_a T} = \frac{(515.4kPa)(6.03x10^{-5}m^3)}{(0.2870 kPa \cdot m^3 / kg \cdot K)(293.15K)} = 0.369 grams \qquad 2)$$

The mass of air that is lost in one pass depends on the mass flow rate, $\dot{m}_a$, out of the air bearings.

$$m_n = \dot{m}_a t \qquad 3)$$

The combined mass flow rate out of the two air bearings used can be calculated using data from the New Way Machine Components website www.newwaybearings.com. The volume flow rates for the 1" flat air bearing and the ¾" I.D. air bushing are given as 1.35 and 8.0 standard cubic feet per hour (SCFH), respectively. This gives a combined total of 9.35 SCFH. To convert SCFH to kg/s, we must multiply by the density of air at 1 atm.

$$\dot{m}_a = (9.35SCFH)\left(1.21\frac{kg}{m^3}\right)\left(\frac{0.3048m}{ft}\right)^3\left(\frac{hr}{3600s}\right) = 8.90x10^{-5}\frac{kg}{s} \qquad 4)$$

Therefore, according to Equation 3, the amount of air the needle must supply is

$$m_n = \left(8.90x10^{-5}\frac{kg}{s}\right)\left(\frac{0.46m}{v_{des}}\right) = \left(\frac{4.09x10^{-5}}{v_{des}}\right)kg. \qquad 5)$$

Now we must calculate the amount of time, t_δ, that the needle will have to supply this mass of air. Assuming that the needle will be engaged with the scanner head for the entire time the head is in contact with the rod, we can use Newton's second law to

calculate t_δ because we have expressions for the acceleration, a, and the acceleration distance, δ_{des}. Although the time it takes to decelerate the scanner head is longer than the time it takes it takes to accelerate it to v_{des} through the distance δ_{des}, we'll use twice this acceleration time, t_a, as a conservative estimate of t_δ. The distance δ_{des} depends on v_{des}, the supply pressure to the cylinder, P_s, the cylinder diameter (d_c = 20 mm), and the masses of the scanner head and the piston (m_s = 782 grams, m_p = 69 grams).[1] We will leave P_s as a variable as well since it depends on v_{des}.

$$\delta_{des} = \frac{2v_{des}^2(m_s + m_p)}{\pi d_c^2 P_s} = \frac{2v_{des}^2(0.782 + 0.069)kg}{\pi(0.020m)^2 P_s} = 1354\frac{v_{des}^2}{P_s}m \qquad 6)$$

The acceleration from 0 m/s to v_{des} can be written as

$$a = \frac{\pi d_c^2 P_s}{4(m_s + m_p)} = \frac{\pi(0.020m)^2 P_s}{4(0.782 + 0.069)kg} = 3.692x10^{-4} P_s \frac{m}{s^2}. \qquad 7)$$

Derivations of Equations 6 and 7 are given in Mr. Butcher's thesis. The acceleration time is given by the equation

$$\delta_{des} = \frac{1}{2}at_a^2. \qquad 8)$$

$$t_a = \sqrt{\frac{2\delta_{des}}{a}} = \sqrt{\frac{2\left(1354\, v_{des}^2 / P_s\right)m}{(3.692x10^{-4} P_s)\, m / s^2}} = 2708\frac{v_{des}}{P_s}s \qquad 9)$$

The total time the needle is engaged, t_δ, is simply two times t_a.

$$t_\delta = 2t_a = 5416\frac{v_{des}}{P_s}s \qquad 10)$$

[1] These values for the masses and the cylinder diameter apply to the previous design and have changed in the new design. However, the analysis is still valid using these values since it yields a conservatively low value for the maximum allowable needle length.

Now we can use this time to solve for the mass flow rate out of the needle as a function of the desired velocity and the supply pressure, $\dot{m}_n (v_{des}, P_s)$. While the needle is engaged, the total mass flow rate into the air tank is $\dot{m}_n - \dot{m}_a$. This mass flow rate is simply equal to the mass of air that the needle must supply divided by the total time the needle is engaged.

$$\dot{m}_n - \dot{m}_a = \frac{m_n}{t_\delta} \tag{11}$$

Since we already found expressions for $\dot{m}_a$, m_n, and t_δ in Equations 4, 5, and 10, we can substitute them into Equation 11 to find an expression for $\dot{m}_n$.

$$\dot{m}_n = \left(\frac{7.54x10^{-9} P_s}{v_{des}^2} + 8.90x10^{-5} \right) \frac{kg}{s} \tag{12}$$

Clearly, this equation has a maximum where the quantity P_s/v_{des}^2 has a maximum. Using Table 2 on p. 31 of Mr. Butcher's thesis, the largest value of this quantity is found to be at v_{des} = 2 m/s and P_s = 30 psig = 47.7 psia = 329.1 kPa. This gives a value for the needle mass flow rate of

$$\dot{m}_n = 7.10x10^{-4} \frac{kg}{s}. \tag{13}$$

There are three parameters that must be selected in order to achieve this mass flow rate. They are the supply pressure to the needle, P_n, the length of the needle, L, and the diameter of the needle, D. I will choose a supply pressure to the needle of 110 psig = 124.7 psia = 859.9 kPa. This should not produce choked flow since the ratio of absolute pressures is greater than 0.528 (Fox, 626).

$$\frac{74.7 psi}{124.7 psi} = 0.599 \geq 0.528 \tag{14}$$

In order to determine values for D and L we must do an energy balance on a control volume that consists of the needle and the supply tank to the needle. Although the flow is actually incompressible, we will treat it as compressible in the following equations since the purpose of this analysis is simply to find suitable dimensions for the needle. By treating the flow as compressible, we overestimate the amount of energy lost from one end of the needle to the other and arrive at needle dimensions that will be sufficient.

Let state 1 correspond to the supply tank at 110 psig and state 2 correspond to the outlet of the needle at 60 psig.

$$\left[\frac{P_1}{\rho_a}+\frac{v_1^2}{2}+gz_1\right]-\left[\frac{P_2}{\rho_a}+\frac{v_2^2}{2}+gz_2\right]=h_{lT}=h_l+h_{lm} \qquad 15)$$

The terms on the right side of the equation are the head losses. The total head loss, h_{lT}, is the sum of the major losses, h_l, and the minor losses, h_{lm}. The major losses are due to friction in the flow and the minor losses are due to bends, area changes and inlet configurations. Assuming that the average velocity in the supply tank is zero and that $z_1 = z_2$, Equation 15 reduces to

$$\frac{P_1-P_2}{\rho_a}-\frac{v_2^2}{2}=h_{lT}=h_l+h_{lm}\,. \qquad 16)$$

We'll use the density of air at 85 psig = 99.7 psia for these equations since 85 psig is exactly in the middle of 60 and 110 psig. From the ideal gas law, the increase in density is directly proportional to the increase in pressure at the same temperature and volume. The density of air at 14.7 psia is 1.21 kg/m^3 (Fox, 707). Therefore, at 99.7 psia the density of air is 8.21 kg/m^3. The average velocity, v, is a function of the cross-sectional area of the needle and the volumetric flow rate, Q.

$$v = \frac{Q}{A} \tag{17}$$

$$Q = \frac{\dot{m}_n}{\rho_a} = \frac{7.10x10^{-4}\, kg/s}{8.21 kg/m^3} = 8.65x10^{-5}\, \frac{m^3}{s} \tag{18}$$

If we choose a needle diameter of 1 mm, then the average velocity becomes

$$v = \frac{Q}{0.25\pi D^2} = \frac{8.65x10^{-5}\, m^3/s}{0.25\pi(0.001m)^2} = 110.1\frac{m}{s}. \tag{19}$$

Now we have evaluated all the terms on the left side of Equation 16 and we must analyze the total head loss. The major head loss can be described by the following equation (Fox, 359).

$$h_l = f\frac{Lv^2}{2D} \tag{20}$$

The friction factor, *f*, is a function of the Reynold's number and the relative roughness, *e/D*. Using a dynamic viscosity of μ = 1.81x10^{-5} Pa·s for air at 293.15 K, the Reynold's number for this flow is

$$\mathrm{Re} = \frac{\rho v D}{\mu} = \frac{(8.21 kg/m^3)(110.1 m/s)(0.001m)}{1.81x10^{-5}\, Pa \cdot s} = 49940. \tag{21}$$

If we assume that the needle will be made of commercial steel, then the roughness, *e*, can be approximated as 0.046 mm (Fox, 359). Therefore, *e/D* = 0.046mm/1mm = 0.046. Using these two values for the Reynold's number and relative roughness, a friction factor *f* = 0.0675 can be obtained from Fig 8.13 (Fox, 360). Therefore, the major head loss can be written as

$$h_l = 0.0675\frac{L(110.1 m/s)^2}{2(0.001m)} = 4.09x10^5 L\frac{m^2}{s^2}. \tag{22}$$

The minor head loss can be described by the following equation (Fox, 362).

$$h_{lm} = K\frac{v^2}{2} \qquad 23)$$

The minor loss coefficient, K, depends on the configuration of the inlet to the needle from the supply. If the edges of that inlet are sufficiently rounded, ($r/D > 0.15$) then $K = 0.04$ (Fox, 363). Since the diameter of this needle is so small, is should be possible to sufficiently round the inlet so that this value of K can be used. Although minor losses this small can usually be neglected, we'll leave it in the equation for added accuracy.

$$h_{lm} = (0.04)\frac{(110.1 m/s)^2}{2} = 242.4\frac{m^2}{s^2} \qquad 24)$$

It should be noted that the average velocity at the outlet of the pipe was used in this equation as in Equation 20 to calculate the head losses. In actuality, the velocity and pressure would vary along the length of the needle, but simply using the outlet velocity in the analysis will overestimate the actual head losses and result in values for the needle dimensions that will be sufficient.

Now, the only unknown in Equation 16 is L, so we can solve for it.

$$\frac{(110 psig - 60 psig)(6895 Pa/psi)}{8.21 kg/m^3} - \frac{(110.1 m/s)^2}{2} = (4.09x10^5 L + 242.4)\frac{m^2}{s^2} \qquad 25)$$

Solving for L gives $L = 0.0873$ m = 3.44 in. Therefore, a needle with a diameter of 1 mm and a length of no more than 87.3 mm supplied with a pressure of 110 psig can supply the scanner head with enough air to operate independent of the tether if one of these needles is at each end of the track.

Initially, attempts were made to purchase two blow gun nozzles to serve as the needles. (Blow gun nozzles are the nozzles commonly used to inflate basketballs or volleyballs.) These nozzles have very small outlet diameters and would have functioned

perfectly for our purposes here. However, no nozzles could be found that satisfied both the length and outlet diameter requirements. Therefore, we decided to machine our own. Our needles were modeled directly from these blow gun nozzles, but the length and diameter were chosen to suit our purposes. For the shafts of the needles, thin stainless steel hypodermic tubing was purchased from Small Parts Inc. This tubing has an inside diameter of 0.038 in. (0.9652 mm) which is very close to 1 mm. A drawing of the needles can be seen on page 69 in Appendix B.

2.1.2 Needle Placement

One check that must be made when deciding where to make the needles engage with the scanner head is to determine the moment that will be created on the air bushing by the air flowing out of the needle. We must determine the maximum allowable distance away from the scanner head's center of gravity at which a needle could be engaged so that the total moment created would not exceed the maximum allowable moment that can be applied to the air bushing.

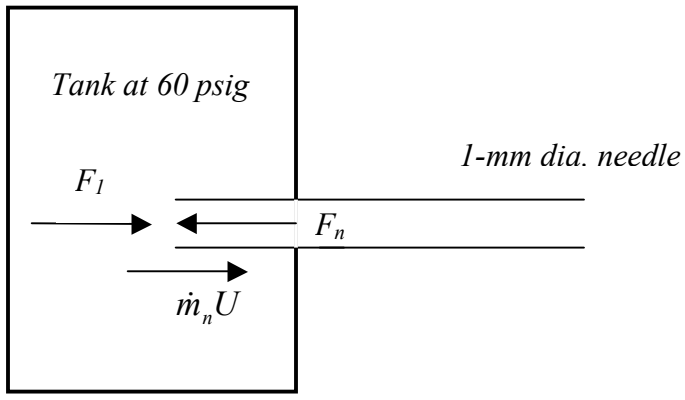

Figure 1 Free-Body Diagram of Tank and Needle Engagement

The air bushing can withstand a maximum moment of 1130 N·mm. (Butcher, 14) Therefore, the sum of the moments caused by the introduction of air from the needle and any eccentricity in the placement of the piston force must be less than this value. We will return to the piston force later and first derive and expression for the force created by the introduction of the air from the needle.

The free-body diagram in Figure 1 shows the needle and the tank engaged. F_1 is the force exerted by the air in the tank on the cross section of the needle opening, and F_n is the force exerted on the tank by the introduction of air from the needle. The other force shown is the needle mass flow rate times the centerline velocity at the needle outlet. We can simply sum the forces to find the relationship of the terms.

$$\sum F = F_n - F_1 = \dot{m}_n U \Rightarrow F_n = F_1 + \dot{m}_n U \qquad 26)$$

We can easily calculate F_1 since we know P_1 = 74.7 psia = 515.4 kPa, and the needle inner diameter is 1 mm.

$$F_1 = P_1 A = (515.4x10^3\, Pa)0.25\pi(0.001m)^2 = 0.405N \qquad 27)$$

The centerline velocity at the needle outlet can be calculated using the following equation (Fox, 354).

$$\frac{v}{U} = \frac{2n^2}{(n+1)(2n+1)} \qquad 28)$$

In Equation 28, v is the average velocity, U is the centerline velocity, and n is given by the following equation.

$$n = -1.7 + 1.8 \log \mathrm{Re}_U \qquad 29)$$

Equations 28 and 29 only apply for fully developed flow, but since the length of the needle (87.3 mm) is greater than 80 diameters, the flow can be assumed to be fully

developed at the outlet (Fox, 334). It should be noted that the Reynold's number in this equation is evaluated at the centerline velocity, U, which is the variable we're trying to solve for. Therefore, the Reynold's number must be left as a function of U for now.

$$\mathrm{Re}_U = \frac{\rho v D}{\mu} = \frac{(8.21 kg/m^3)(U\, m/s)(0.001m)}{1.81x10^{-5}\, Pa \cdot s} = 454U \qquad 30)$$

If we substitute this expression for the Reynold's number into Equation 29, then we can solve Equations 28 and 29 simultaneously for U and n (the average velocity, v, is known to be 110.1 m/s). This gives values of n = 6.92 and U = 135.1 m/s. Now we can solve for F_n using Equation 26.

$$F_n = F_1 + \dot{m}_n U = 0.405N + (7.10x10^{-4}\, kg/s)(135.1 m/s) = 0.501N \qquad 31)$$

Now we can sum the applied moments and solve for the maximum allowable distance away from the center of gravity that the needle could be placed.

$$\sum M = r_p F_p + r_n F_n \qquad 32)$$

In this equation, F_p is the force exerted by the piston, r_p is the distance from the center of gravity to where the piston force is applied, and r_n is the distance from the center of gravity to where the needle engages. This sum must be less than or equal to 1130 N·mm. For purposes of this calculation, we will use the largest value of the force exerted by the piston. This force is 125.3 N and it occurs when v_{des} = 5 m/s and the supply pressure is 77 psig. We will also select a conservative value of 6 mm for r_p even though it is possible to apply the piston force more accurately than that.

$$\sum M = (6mm)(125.3N) + r_n(0.501N) = 1130N \cdot mm \qquad 33)$$

Solving this equation gives r_n = 754.9 mm. This is the maximum distance from the center of gravity that the needle could be made to engage with the tank. Keep in mind

that this distance will increase as the piston force is applied more accurately. Therefore, we can safely say that the force caused by the introduction of air into the tank will not cause an excessive moment on the air bushing.

2.2 Energy Replacement

As we know, in order to achieve continuous operation of the system, the energy that is continually lost must somehow be replaced. In the previous design, all of the energy needed for the system was supplied by the pneumatic cylinders. This was a rather inefficient method, and the new design features a more efficient method of energy replacement. This involves precharging a small volume of air on the rod side of the cylinder to a certain pressure. When the scanner head initially impacts the rod, that small volume will expand and the pressure will therefore decrease. This expansion process will actually do work which is equivalent to adding energy to system. In addition to this new method, two new cylinders were also purchased. These are Pyrex glass cylinders from the Airpot Corporation. They have a bore of 15.9 mm and a stroke of 100 mm. A piston was included with each, but we had to design and manufacture our own rods and housings as will be discussed in Section 2.4. These pneumatic cylinders are precision-machined so that no seals are required around the piston which greatly reduces the friction in the cylinder. Less friction means that less energy is lost and therefore less energy must be replaced.

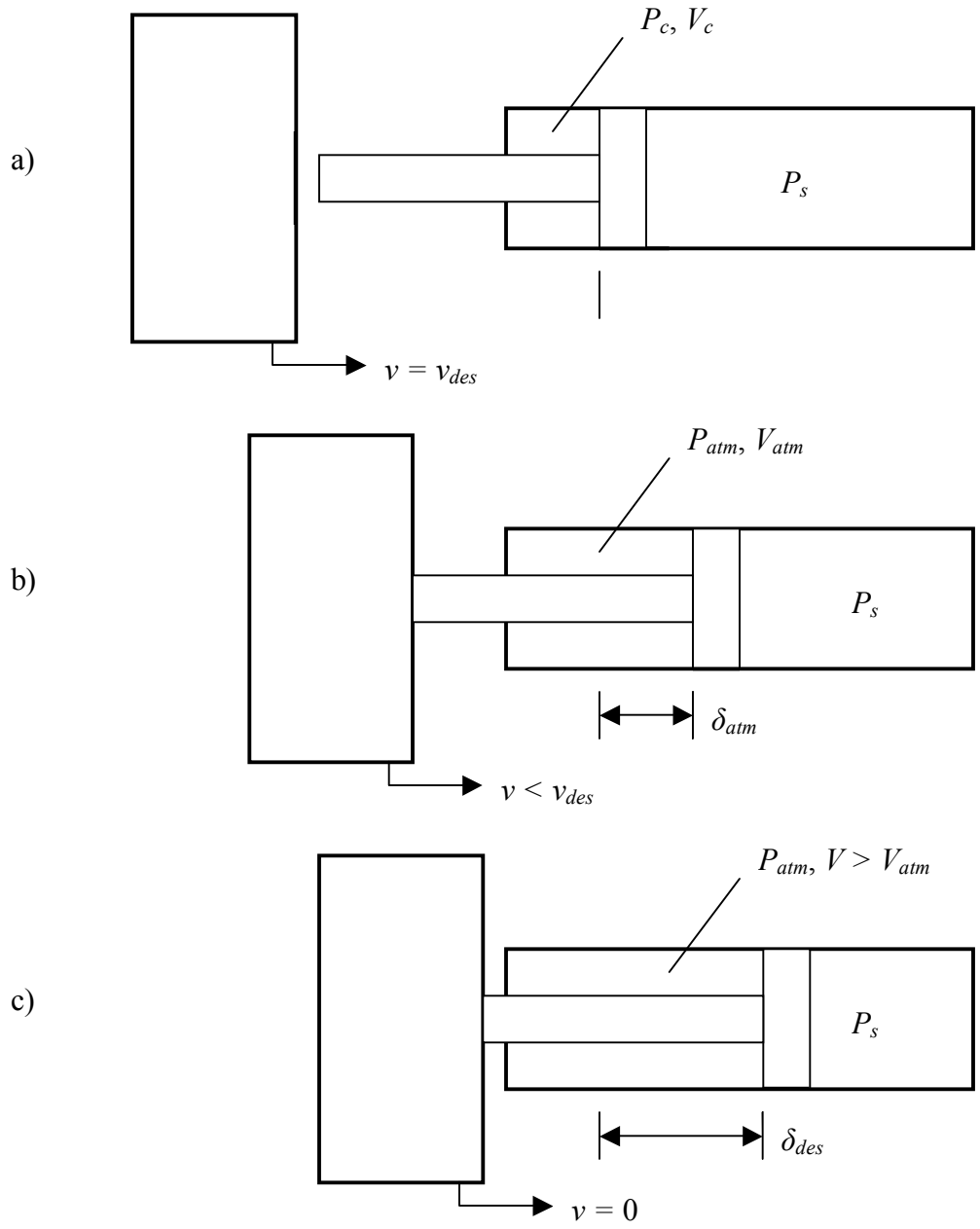

Figure 2 Expansion of Precharge Volume: a) precharge volume immediately prior to scanner head impact, b) precharge volume reaches atmospheric pressure, c) apex of deflection

Figure 2 above shows the details of the expansion process. Figure 2a shows the system immediately prior to the impact of the scanner head and the rod. At this time the volume on the rod side is equal to the precharge volume, V_c, and it has already been pressurized to the precharge pressure, P_c. When the scanner head impacts the rod, the volume on the rod side begins to expand and the pressure decreases. Figure 2b shows the system when the volume has reached the critical level, V_{atm}, where the pressure is equal to atmospheric. The distance that the piston has been deflected to reach this point is denoted by δ. At this time, a valve is opened to the atmosphere. This allows the pressure to remain at atmospheric while the scanner head continues to deflect the piston. Figure 2c shows the scanner head at zero velocity at the apex of deflection. At this point, the pressure differential across the piston will force the head back in the opposite direction. The valve will remain open to the atmosphere so that as the volume on the rod side decreases, air can be expelled and the pressure will still remain at atmospheric. While the scanner head is traveling down and back along the track, the valve will close and the rod side will be pressurized to P_c to await the next impact. The details of how this is accomplished are discussed in Section 2.2.3. The following sections discuss the calculation of the precharge volume and pressures.

2.2.1 System Losses

As described above, the purpose of pressurizing a certain volume of air on the rod side of the cylinder prior to impact is that the expansion of that air adds energy to the

system equal to the energy lost during the previous pass. By this method, the cylinder will actually function more like a pneumatic spring instead of having to supply all the energy required to propel the scanner head in the opposite direction. In order to determine a precharge pressure and volume that are appropriate, we must first evaluate the amount of energy that was lost in that pass. The two major energy losses are due to momentum transfer between the scanner head and the rod and friction inside the cylinder. By determining expressions for these two losses, we can calculate a volume at a certain pressure, the expansion of which to atmospheric pressure will do an amount of work equal to those losses.

We will start by designating a value for the precharge pressure equal to 70% of the supply pressure ($0.7P_s$). Also, we can assume that the expansion of the precharge volume can be considered isentropic since it occurs over such a short time that the net mass flow to the volume is approximately zero. Leak-rate data was obtained from the Airpot Corporation website. Calculations using this data showed that at 5 m/s, roughly 0.0056 mL of air would leak around the piston during the rebound time and roughly 0.0085 mL would leak during one pass down the track. These small volumes of air are less than 0.5% of the total precharge volume of 1570 mm^3 (see Table 1) so the energy lost due to leakage can be neglected.

Momentum Transfer:

Right before the scanner head impacts the rod, it is traveling at a velocity v_{des}. It impacts the rod and they start traveling together at a velocity v_1. We can relate these two

velocities using the law of conservation of momentum where m_s and m_p are the masses of the scanner head and the piston/rod, respectively.

$$m_s v_{des} = (m_s + m_p)v_1 \Rightarrow v_1 = \frac{m_s v_{des}}{(m_s + m_p)} \tag{34}$$

The above equation assumes that the impact is perfectly plastic since both bodies are given the same final velocity before the gases inside the cylinder have been fully compressed. In actuality, the impact is not completely plastic. However, the coefficient of restitution can be assumed to be zero because, for engineering purposes, the head and the piston/rod have reached essentially the same velocity.

To find the energy lost due to this momentum transfer, we can subtract the final kinetic energy from the initial kinetic energy.

$$\frac{1}{2}m_s v_{des}^2 - \frac{1}{2}(m_s + m_p)\left(\frac{m_s v_{des}}{(m_s + m_p)}\right)^2 = \frac{1}{2}\left(\frac{m_s m_p}{m_s + m_p}\right)v_{des}^2 \tag{35}$$

The total energy lost to due to momentum transfer, L_m, is actually twice this expression because when the scanner head rebounds, the supply pressure must accelerate the piston, rod, and head to the desired velocity instead of just the head. Therefore, the total energy lost due to momentum transfer can be expressed as

$$L_m = \left(\frac{m_s m_p}{m_s + m_p}\right)v_{des}^2 . \tag{36}$$

This equation illustrates the need to minimize the mass of the rod and piston. The description of the design of the rod is given in Section 3.1.3.

Piston Friction:

On the Airpot Corporation website, www.airpot.com, the force of piston friction is said to be 1-2% of the piston load for all their cylinder models. The piston load is simply the supply pressure, P_s, times the effective area of the piston. The effective piston area is also given by Airpot and we will call it f_p. If we assume the maximum friction of 2% of the load, the force of piston friction, F_f, can be written as follows.

$$F_f = 0.02 f_p P_s \tag{37}$$

To determine the energy lost due to friction, L_f, we must multiply this force by the total distance over which it's acting which is $2\delta_{des}$.

$$L_f = F_f(2\delta_{des}) = 0.02 f_p P_s \left(\frac{4 v_{des}^2 (m_s + m_p)}{\pi d_c^2 P_s} \right) = \frac{0.08 f_p v_{des}^2 (m_s + m_p)}{\pi d_c^2} \tag{38}$$

Now the energy losses due to friction can be quantified as well.

2.2.2 Precharge Volume

Now that we have expressions for the energy losses, let's derive an expression for the work done in the expansion process. This expression will be equated to the sum of Equations 36 and 38 to determine the precharge volume. As stated above, we can assume that the expansion is isentropic since it occurs over such a short time that the net mass flow to the volume can be approximated as zero. The equation for isentropic expansion of air is $PV^{1.4}$ = constant. The amount of work done in an expansion process is (Shapiro, 46)

$$W = \int_{V_1}^{V_2} P dV \,. \tag{39}$$

From the isentropic expansion equation we can write the following.

$$PV^{1.4} = C \Rightarrow P = CV^{-1.4} \tag{40}$$

If we substitute this into the work equation, we can carry out the integration.

$$W = \int_{V_1}^{V_2} CV^{-1.4} dV = -\frac{C}{0.4}(V_2^{-0.4} - V_1^{-0.4}) \tag{41}$$

In our problem, the initial volume is the precharge volume, V_c, and the final volume is the volume at which the pressure reaches atmospheric, V_{atm}. We can write the previous equation simply in terms of V_c if we make three substitutions. Let $V_1 = V_c$, and write C and V_2 in terms of V_c. From the isentropic expansion equation we have

$$P_c V_c^{1.4} = 0.7 P_s V_c^{1.4} = C = P_{atm} V_{atm}^{1.4} \tag{42}$$

From this equations we can write

$$C = 0.7 P_s V_c^{1.4} \tag{43}$$

and

$$V_2 = V_{atm} = \left(\frac{0.7 P_s}{P_{atm}} \right)^{5/7} V_c . \tag{44}$$

By making these substitutions, Equation 41 can be written as follows.

$$W = -\frac{7}{4} P_s V_c^{1.4} \left(\left(\frac{0.7 P_s}{P_{atm}} \right)^{-2/7} - 1 \right) V_c^{-0.4} = \frac{7}{4} P_s V_c \left(1 - \left(\frac{0.7 P_s}{P_{atm}} \right)^{-2/7} \right) \tag{45}$$

Now we want to equate this expression with the total energy lost, $L_m + L_f$. Therefore, by setting Equation 45 equal to the sum of Equations 36 and 38 and simplifying, we get the following.

$$\frac{7}{4} P_s V_c \left(1 - \left(\frac{0.7 P_s}{P_{atm}} \right)^{-2/7} \right) = \left(\frac{m_s m_p}{m_s + m_p} + \frac{0.08 f_p (m_s + m_p)}{\pi d_c^2} \right) v_{des}^2 \tag{46}$$

Solving for V_c gives

$$V_c = \frac{4}{7P_s}\left(1-\left(\frac{0.7P_s}{P_{atm}}\right)^{-2/7}\right)^{-1}\left(\frac{m_s m_p}{m_s+m_p}+\frac{0.08 f_p (m_s+m_p)}{\pi d_c^2}\right)v_{des}^2 \qquad 47)$$

Substituting this into Equation 44 also gives an expression for V_{atm}.

$$V_{atm} = \left(\frac{0.7P_s}{P_{atm}}\right)^{5/7}\frac{4}{7P_s}\left(1-\left(\frac{0.7P_s}{P_{atm}}\right)^{-2/7}\right)^{-1}\left(\frac{m_s m_p}{m_s+m_p}+\frac{0.08 f_p (m_s+m_p)}{\pi d_c^2}\right)v_{des}^2 \qquad 48)$$

Now we have expressions for the initial and final volumes such that the work done in expanding from one to the other will be equal to the energy lost due to momentum transfer and piston friction. As a final check, we need to make sure that the distance that the piston must displace to go from V_c to V_{atm} is less than δ_{des} so that the pressure will actually get to atmospheric before the scanner head reaches zero velocity. The final volume is the sum of the initial volume and the additional volume created by displacing the piston. That additional volume can be written as

$$f_R \delta_{atm} = V_{atm} - V_c \qquad 49)$$

where f_R is the effective area on the rod side of the cylinder, and δ_{atm} is the distance the piston must displace to get the pressure to reach atmospheric. We can simply solve Equation 49 for δ_{atm}.

$$\delta_{atm} = \frac{V_{atm} - V_c}{f_R} \qquad 50)$$

In order to reach atmospheric pressure before the scanner head reaches zero velocity, δ_{atm} must be less than or equal to δ_{des}.

$$\frac{V_{atm} - V_c}{f_R} \le \frac{2v_{des}^2 (m_s+m_p)}{\pi d_c^2 P_s} \qquad 51)$$

If this inequality is not satisfied, then a different precharge pressure must be selected and used to solve for different initial and final volumes until the inequalilty is satisfied.

Obviously, as v_{des} varies from 2 m/s to 5 m/s either P_s, V_c, or both would have to change to satisfy the above equations. There are several ways that this system of precharging air on the rod side can be applied to the different desired velocities. The simplest method would be to only vary one of those two parameters and hold the other one constant. The supply pressure is the easiest to vary since is simply involves adjusting the regulator. Therefore, the system was designed to have a constant precharge volume. The precharge volume in the new design (which will be described more in Section 2.2.3) consists of a small volume on the rod side of the cylinder, the channel connecting that volume to the cavity of the new valve, the cavity, and the connection between the cavity and the solenoid valve. The sum of these volumes is approximately equal to 1570 mm^3.

The following table, Table 1, shows the precharge volume data for the new design. The supply pressures were calculated by assuming the value of 1570 mm^3 for V_c and then using Equation 47 to solve for P_s for each of the desired velocities. Equation 44 was then used to calculate V_{atm} for each of the cases. The two distances δ_{atm} and δ_{des} are also tabulated to show that the volume will, in fact, reach V_{atm} in each of the cases before the scanner head reaches the apex of deflection. Equations 50 and 6 were used to calculate these values of δ_{atm} and δ_{des}, respectively.

Table 1 Precharge Volume Data

P_s (psig)	v_{des} (m/s)	V_c (mm^3)	V_{atm} (mm^3)	δ_{atm} (mm)	δ_{des} (mm)
21.1	2	1570	2271	4.25	26.3
40.0	3	1570	2908	8.11	41.9
53.5	4	1570	3631	12.5	54.6
76.1	5	1570	4414	17.2	65.0

2.2.3 New Valve Design

The pressurization of this precharge volume obviously requires some sort of valve to dispense the air into it. However, the particular way that the air must be able to flow out of this volume required something a little more complex that the ordinary poppet valve. Specifically, the way that the valve must pop open when the volume reaches atmospheric pressure and remain open even after the piston starts to move back in the opposite direction. When the piston moves back in the other direction it must expel the air on the rod side to the atmosphere, but a normal poppet valve would close in this situation and not let that happen. In addition, for this application it is necessary for the inlet and outlet areas to be different, which is not the case with a normal poppet valve. To solve this problem, a new valve was designed to allow the air to exit the precharge volume in the necessary manner. This valve is used in conjunction with another commercially available valve that dispenses the air into the precharge volume to begin

with. We will begin by discussing the valves that were purchased and then describing how the new valves were designed.

In order to achieve the addition of the air into the precharge volume, two miniature solenoid valves were purchased from The Lee Company. There were a wide variety of these valves to choose from each with different available flow rates. The flow rates of the different valves were described by a unit of measurement that The Lee Company defined called the "Lohm" (L*iquid* ohm). This was defined as the resistance to fluid flow just as an ohm is defined as the unit of resistance to current in an electrical system. The equation relating the fluid flow restriction (during sonic flow) of a certain valve to the other system parameters is given as

$$Lohms = \frac{Kf_T P_1}{Q} \qquad 52)$$

where K is the units constant, f_T is the temperature correction factor, P_1 is the upstream absolute pressure, and Q is the mass flow rate through the valve. The temperature correction factor is simply unity if the system is operated at room temperature, which it is in this case. The units constant is simply a conversion factor. For ease of calculation, any types of units can be used for the pressure and mass flow rate and the necessary conversion factor, K, can be read from a table given on The Lee Company website.

The valve that was selected for this project was the INKX0511400A VHS – 25+ Nanoliter Dispensing Valve. This valve has an open-liquid flow restriction of 4750 Lohms. A drawing of the valve is shown in Figure 3.

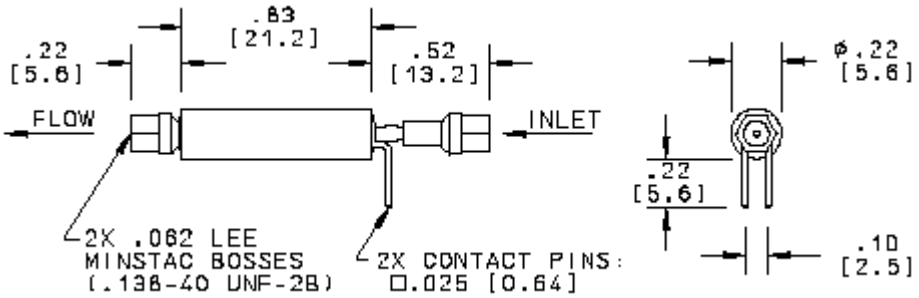

Courtesy of The Lee Company

Figure 3 The INKX0511400A VHS – 25+ Nanoliter Dispensing Valve

Before choosing this valve, it was necessary to determine if the flow rate would be sufficient to transfer enough air into the precharge volume in the available time for each of the different desired velocities. The mass flow rate through the valve for a given supply pressure can be calculated using Equation 52, and then we can determine if that flow rate is sufficient to achieve the required precharge pressure before the scanner head makes it all the way down to the other end of the track and back.

If we can show that the mass flow rate is sufficient at the two limiting cases (v_{des} = 2 m/s and v_{des} = 5 m/s) then we can assume that it will also be sufficient at any desired velocity in between. We will start with the case where v_{des} = 2 m/s. The required supply pressure for this desired velocity is P_s = 21.4 psig = 36.1 psia. If we want to get a value for the mass flow rate in kg/s, then the corresponding units constant is found to be K = 0.0055 (kg/s)/psia. Equation 52 gives

$$Q = \frac{Kf_T P_1}{Lohms} = \frac{\left(0.0055\frac{kg/s}{psia}\right)(1)(36.1 psia)}{4750} = 4.18x10^{-5}\, kg/s. \qquad 53)$$

Now we need to know how much air needs to be transferred into the precharge volume. This can be calculated using the ideal gas law. Assuming that state 1 is the precharge volume initially at atmospheric pressure and state 2 is the precharge volume at the necessary pressure of $0.7P_s$, the ideal gas law reduces to

$$\frac{P_1}{m_1} = \frac{P_2}{m_2}. \tag{54}$$

The initial and final pressures are P_1 = 14.7 psia and P_2 = 0.7(36.1 psia) = 25.3 psia. The initial mass of air in the precharge volume is found by multiplying the precharge volume by the density of air at atmospheric pressure.

$$m_1 = V_c \rho_a = (1350x10^{-9} m^3)(1.21 kg/m^3) = 1.634x10^{-6} kg \tag{55}$$

Therefore, the final mass of air in the precharge volume is

$$m_2 = \frac{P_2}{P_1} m_1 = \frac{25.3 psia}{14.7 psia}(1.634x10^{-6} kg) = 2.811x10^{-6} kg \tag{56}$$

This means that the amount of air that must be transferred to the precharge volume is $m_2 - m_1 = 1.177x10^{-6}$ kg. The valve must be able to supply this much air before the scanner head goes all the way up and down the track. The total length of the scanning path is 46 cm, so going down and back would cover a distance of 92 cm. We can simply approximate the total travel time as $2t$ = 2(0.92 m/(2 m/s)) = 460 ms. (This conservative approximation disregards the acceleration in the rebound process and assumes constant velocity during that period.) The amount of time that the valve requires to supply $1.177x10^{-6}$ kg of air with a supply pressure of 36.1 psia is given by the following equation.

$$t_c = \frac{\Delta m}{Q} = \frac{1.177x10^{-6} kg}{4.18x10^{-5} kg/s} = 28.2 ms \tag{57}$$

Since this time is far less that 460 ms, there is sufficient time for this valve to supply the necessary amount of air in the case where v_{des} = 2 m/s. Using the same method, it can be shown that for the other limiting case (v_{des} = 5 m/s) the total travel time is approximately 184 ms and t_c = 51.9 ms. Therefore, by showing that this valve with an open-liquid flow restriction of 4750 Lohms is sufficient in each of the limiting cases, we have shown that it is sufficient for all cases in between.

Now we can describe how the new valve that is used in conjunction with the miniature solenoid valve was designed. Initially, we knew that the valve had to function as follows:

- Remain closed while the volume is being pressurized
- Pop open when the volume reaches atmospheric pressure and let air flow in to keep the pressure constant
- Remain open while the scanner head is propelled in the opposite direction and allow air to flow out of the volume
- Close so that the process can be repeated

The way that this operation was achieved is shown in Figure 4. As can be seen, the design consists of a small cavity that is open to the atmosphere on the top. Inside this cavity is a flat thin disk. The outlet of the miniature solenoid valve is connected to the bottom of the cavity and there is another outlet from the cavity connected to the rod side of the cylinder.

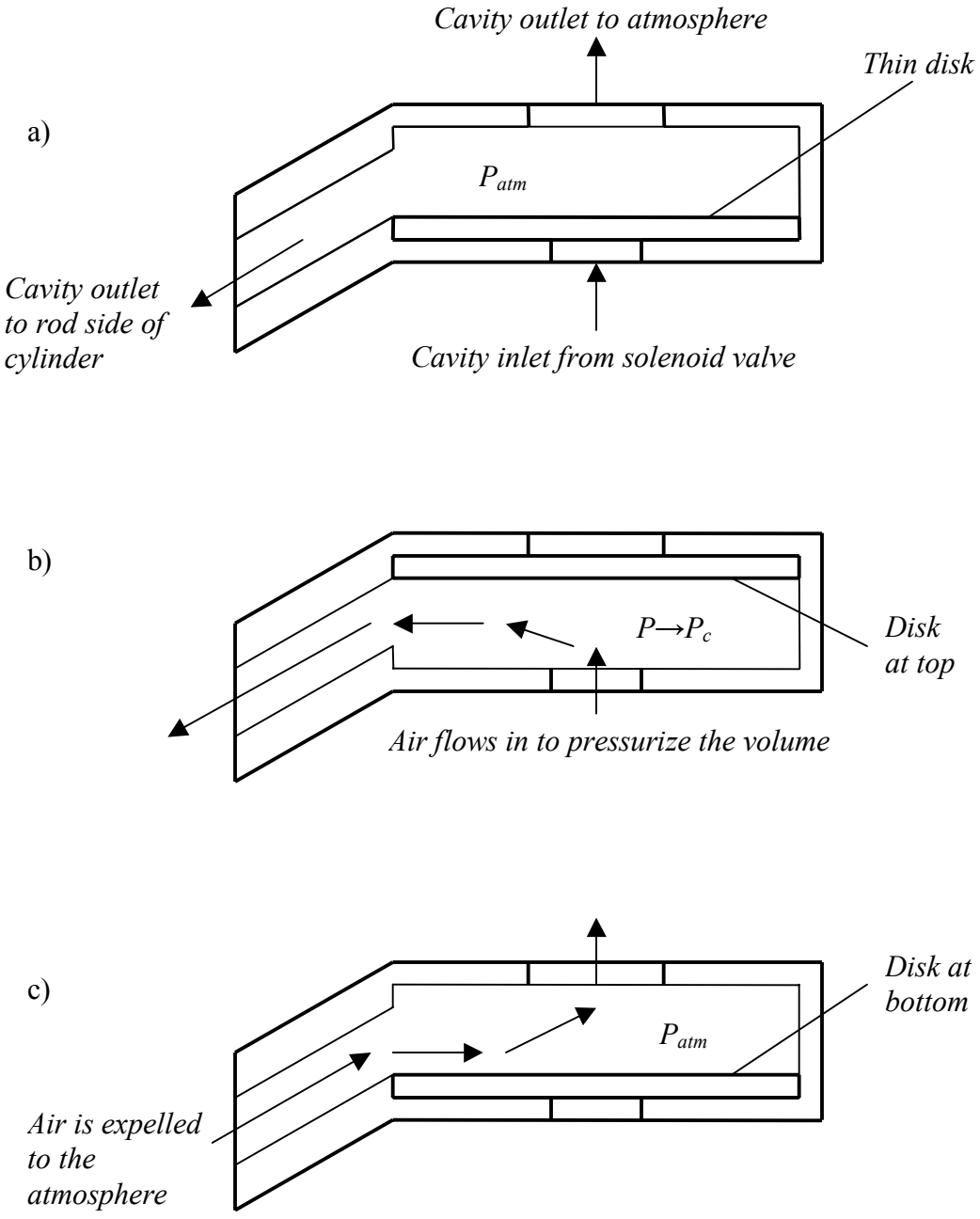

Figure 4 New Valve Operation a) before the precharge volume has been pressurized, b) while the precharge volume is being pressurized, c) after the apex of deflection when air is being expelled from the precharge volume

Initially, the disk simply rests at the bottom of the cavity due to gravity as shown in Figure 4a. When the disk is in this position, the precharge volume is actually open to the atmosphere, so it is at atmospheric pressure. When the solenoid valve opens and begins to supply air to the volume, the force of this flowing air pushes the disk to the top of the cavity blocking the outlet to the atmosphere. Since this outlet is blocked, the pressure in the volume increases. This is shown in Figure 4b. The solenoid valve closes after the appropriate amount of air has been supplied to the volume to get it to reach the precharge pressure, P_c. The disk remains at the top of the cavity since the pressure below it is greater than the pressure above it. The valve remains in this state in preparation for the scanner head impact.

When the scanner head impacts the rod, the volume increases and the pressure begins to decrease as described earlier. When the pressure reaches atmospheric, there is no longer a pressure gradient to keep the disk at the top of the cavity and it falls back to the bottom due to gravity. This connects the precharge volume directly to the atmosphere which obviously maintains it at a constant pressure while the head continues to deflect the piston. After the head has reached the apex of deflection it begins to move back in the opposite direction. During this time, air is forced out of the volume through the cavity and it still remains at atmospheric pressure. This is shown in Figure 4c.

2.3 Vibration Isolation

As described earlier, the rapid oscillations of the scanner head and the repeated impacts with the pneumatic cylinders in the previous design caused significant vibration of the table on which it was mounted. Several methods of reducing the undesirable vibration effects were considered. One method involved mounting the cylinders on two grounded structures separate from the table the track is mounted on. This did not seem convenient since the optical table on which the track was mounted was too much wider than the track to allow for separate structures to be placed directly at each end of the track where the cylinders need to be. Another method involved mounting the entire system on a much more massive table, but preliminary calculations showed that the required mass was prohibitively large.

The method chosen to isolate the system vibrations was to have the scanner track and the cylinders mounted on separate objects. The scanner track was mounted on the table and the cylinders were mounted to a much more massive structure which was suspended above the track. This massive, suspended structure was also mounted to the table, but it doesn't transmit nearly as much force to the table as the previous design. The only force transmitted to the table is due to the lateral motion of the suspended mass, which is very small. By greatly reducing the force on the table, the resulting vibration of the table was also greatly reduced.

In order to determine the parameters of this new suspended mass design, it was first necessary to create a model of the proposed system. This model is shown in Figure 5. It includes the scanner head, M_1, and the larger mass, M_2. It also shows the larger

mass attached to the ground (table) by a damper and a spring. The pieces used to suspend the mass collectively function as the spring since they tend to return the mass to its natural position after it has been displaced.

It should be noted that the piecewise-linear model that is shown in the following figures could have potentially been very difficult to analyze and result in a chaotic system. Depending on the system parameters, it may diverge or otherwise never reach a steady state. Systems very similar to this have been studied extensively and many books have been written on the subject of chaotic systems (*Chaotic and Fractal Dynamics: An Introduction for Applied Scientists and Engineers* or *Chaotic Vibrations: An Introduction for Applied Scientists and Engineers* both by Francis C. Moon). However, in the analysis that follows, it will be shown that suitable system parameters were chosen such that the system converges to a steady state and is not chaotic.

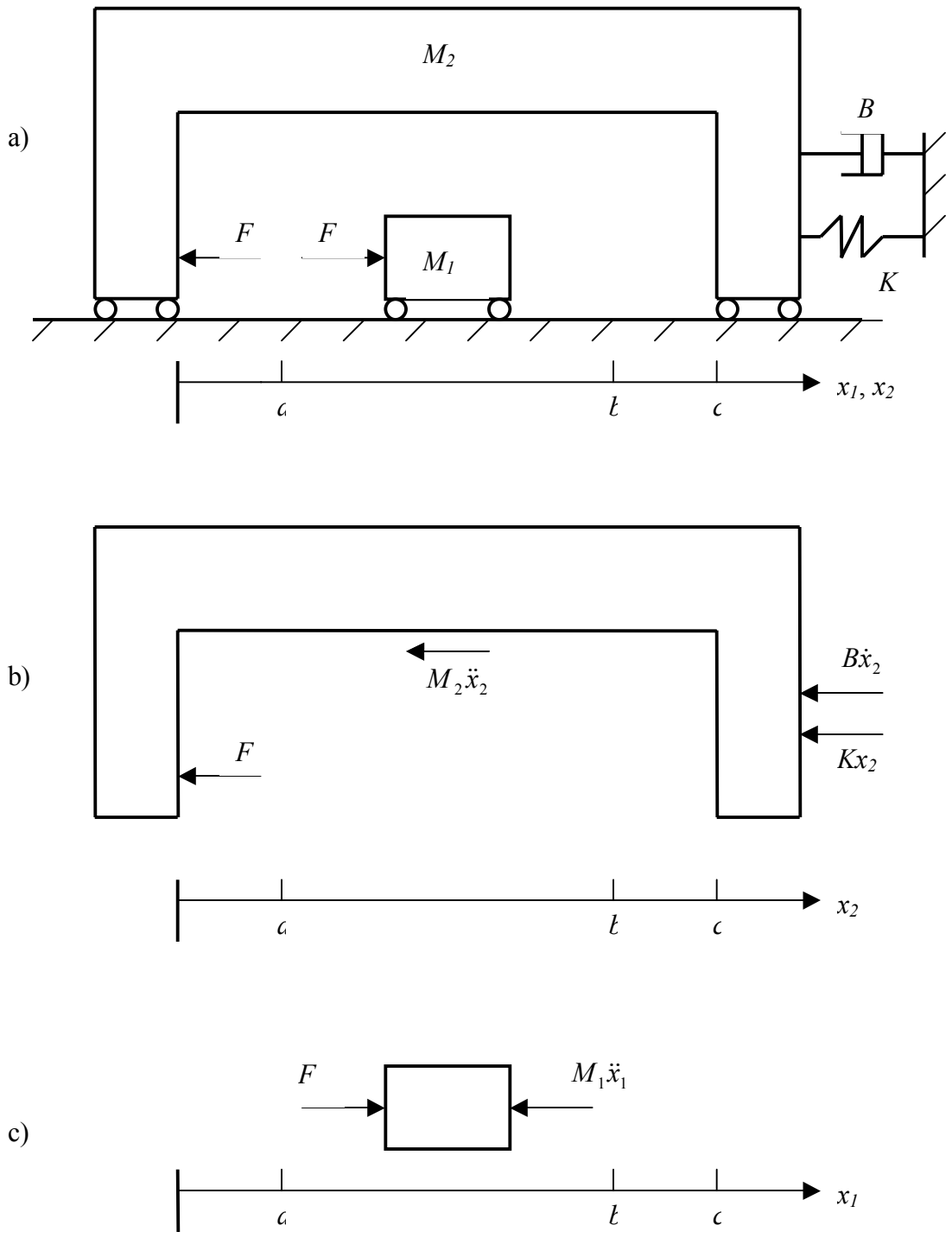

Figure 5 Vibration Isolation System a) System Model, b) Free-Body Diagram of M_2, c) Free-Body Diagram of M_1

2.3.1 Inertial Mass Concept

The force F is the force that the cylinder exerts on the scanner head to accelerate it up to v_{des}. The distance a is the value of δ_{des} for the given desired velocity. The distance from a to b is the length of the scanning path which is 46 cm. The distance from b to c is δ_{des} at the other end of the track. Therefore, the distance from 0 to c is the entire length over which the scanner head travels. In the following analysis, we will consider the state at which the largest vibrations would occur: a desired velocity of 5 m/s. This is the state where the supply pressure and, consequently, the force from the cylinder are the largest. When v_{des} = 5 m/s, the force F takes a value of F_p = 123.9 N since the supply pressure is at 76.1 psig (see Table 1).

From the free-body diagrams in Figures 5b and 5c, the equations of motion for the two masses can easily be found to be

$$M_1\ddot{x}_1 = F \tag{58}$$

$$M_2\ddot{x}_2 + B\dot{x}_2 + kx_2 = -F \tag{59}$$

When the relative position of the head and larger mass is between 0 and a, the force F = F_p. When the relative position is between b and c, F = -F_p. Otherwise, F = 0. We already know the mass of the scanner head is 0.635 kg, so we need to determine values for M_2, B, and k such that the natural frequency of the larger mass is much smaller than the natural frequency of the scanner head while keeping the mass of M_2 as small as possible for practical purposes.

First we must determine the natural frequency of the scanner head. The amount of time that it takes the scanner head to complete one period can be calculated by the following equation

$$T_1 = 4t_a + \frac{2L_1}{v_{des}} \tag{60}$$

where t_a is the time it takes to accelerate the head up to v_{des} through the distance δ_{des} and L_1 is the length of the scanning path. We know from Table 1 that if v_{des} = 5 m/s, δ_{des} = 65 mm; then the period becomes

$$T_1 = 4\sqrt{\frac{2(0.065m)}{123.9N/0.635kg}} + \frac{2(0.46m)}{5m/s} = 0.2872s. \tag{61}$$

Therefore, the natural frequency of the scanner head is $2\pi/T_1$ = 21.9 rad/s. We want the larger mass to have a natural frequency, ω_n, of at most 10% of the scanner head's natural frequency, or no more than 2.2 rad/s. The general form of the characteristic equation (CE) for a second-order system can be used to determine the parameters needed to achieve a certain damping ratio and natural frequency. The general form of the CE and the CE for M_2 are given by the following equations.

$$s^2 + 2\xi\omega_n s + \omega_n^2 = 0 \tag{62}$$

$$s^2 + \frac{B}{M_2}s + \frac{k}{M_2} = 0 \tag{63}$$

By equating the coefficients in Equations 62 and 63, we have two equations for M_2, B, and k in terms of the damping ratio ξ and the natural frequency ω_n.

$$k = M_2\omega_n^2 \tag{64}$$

$$B = 2\xi\sqrt{kM_2} \tag{65}$$

Since there are five variables in these two equations, we must select three of the parameters and solve for the other two. We will select M_2, ω_n, and ξ and solve for the spring and damping constants.

2.3.2 System Model and Simulation

In order to determine what values to select for M_2, ω_n, and ξ, it is necessary to simulate the system model to show that these values produce a desirable output response. Namely, that the resulting forces on the table are low, since large forces are what cause the vibration. By writing the equations of motion (Equations 58 and 59) in state-space form, the system can be easily modeled in Matlab. If we let the position and velocity of each mass be the four state variables, ($q_1 = x_1$, $q_2 = x_2$, $q_3 = \dot{x}_1$, $q_4 = \dot{x}_2$) then the state-space form of the system is

$$\dot{\vec{q}} = \begin{bmatrix} 0 & 0 & 1 & 0 \\ 0 & 0 & 0 & 1 \\ 0 & 0 & 0 & 0 \\ 0 & -k/M_2 & 0 & -B/M_2 \end{bmatrix} \vec{q} + \begin{bmatrix} 0 \\ 0 \\ 1/M_1 \\ 1/M_2 \end{bmatrix} F . \qquad 66)$$

Using Matlab, this system was discretized and a function was written to plot the positions and velocities of M_1 and M_2 as well as the force exerted on the table. The code is given in Appendix A. When the simulation was ran, the damper would actually take energy out of this system until it reached a steady-state value of $\vec{q} = 0$. In order to compensate for this, the velocity of the scanner head was set equal to v_{des} whenever it moved into the region between a and b (relative to the suspended mass). Also, the appropriate velocity was added to M_2 as required by momentum conservation. In effect,

this added a little bit of energy to the system on each pass to make up for the energy being taken out by the damper.

After repeatedly running this simulation, satisfactory values for M_2, ω_n, and ξ were selected using a trial and error method. A mass of M_2 = 100 lb. = 45.36 kg was chosen and a natural frequency of 1.7 rad/s was selected which is only approximately 7.8% of the scanner head's natural frequency. This resulted in a spring constant of k = 131.1 N/m. It was decided that the system would be undamped ($\xi = B = 0$) since this had little effect on the output of the system and it made construction easier due to the fact that no damper had to be incorporated into the design.

The output plots from the Matlab simulation are shown in Figures 6 and 7. The results shown in the figures seem to make intuitive sense. The position of the scanner head oscillates between 0 and 0.59 m, and its velocity goes between -5 and 5 m/s. After about 20 seconds, the oscillation of M_2 reaches steady-state and varies from about -4 to 4 mm. (The scale on the x-axis of this plot is larger than the others to show how long M_2 takes to reach steady-state oscillation.) Also, the velocity of M_2 is very small, only varying between about -0.7 and 0.7 m/s. The force exerted on the table by the suspended mass is shown in Figure 7. Again, this oscillating force takes about 20 seconds to reach steady-state, at which point it has a maximum value of only ±0.5 N. This is tremendously smaller than the force exerted by the cylinder, 123.9 N, which was entirely transmitted to the table in the previous design.

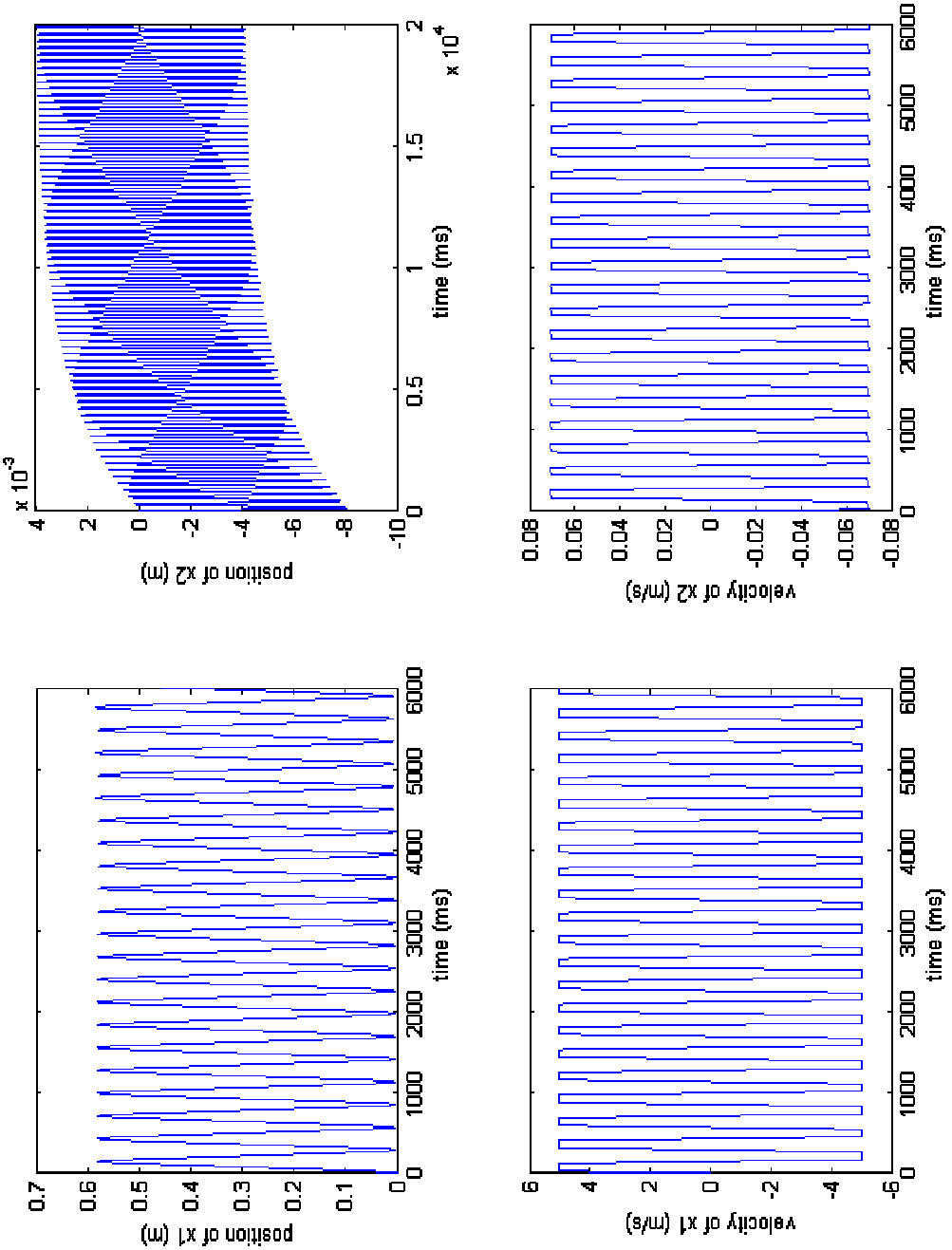

Figure 6 Positions and Velocities of M_1 and M_2 vs. Time

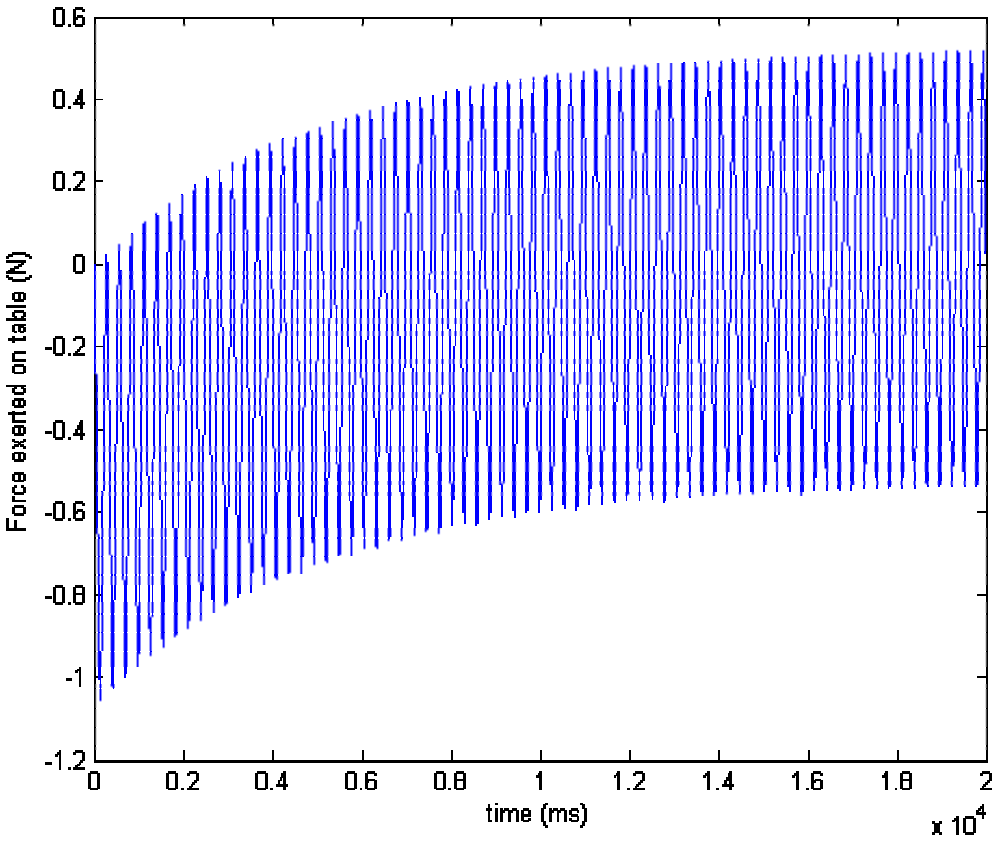

Figure 7 Force Exerted on the Table vs. Time

In the system model shown above in Figure 5a, the large mass is not shown to be suspended, but is attached to ground through a spring (and a damper, but we already chose to make the system undamped). However, in the actual design, the large mass is suspended above the track by four strips of spring steel. Collectively, these strips of steel serve the same function as the spring in the model, and therefore, their dimensions had to be chosen accordingly. They had to be chosen so that the natural deflection of the strips would provide the same resistance to displacement as a spring with a spring constant of

131.1 N/m. In addition to the deflection of the strips, the pendulum effect also tends to return the large mass to the neutral position.

Since there are four strips of spring steel used, each one had to be designed to have an equivalent spring constant of 32.78 N/m. Each of the strips is bolted at both the top and bottom, when means that both ends are restricted from rotation as shown in Figure 8. The total length of the strip is denoted by L_s in Figure 8a. In order to simplify the analysis, the strip can actually be divided into two equal parts that can be treated as rectangular beams with one free end. The equation for the deflection of a beam is (Gere p 882)

$$\delta = \frac{PL^3}{3EI} \qquad 67)$$

where P is the force applied to the end of the beam, L is the length of the beam, E is the elastic modulus of the material, and I is the moment of inertia of the cross section.

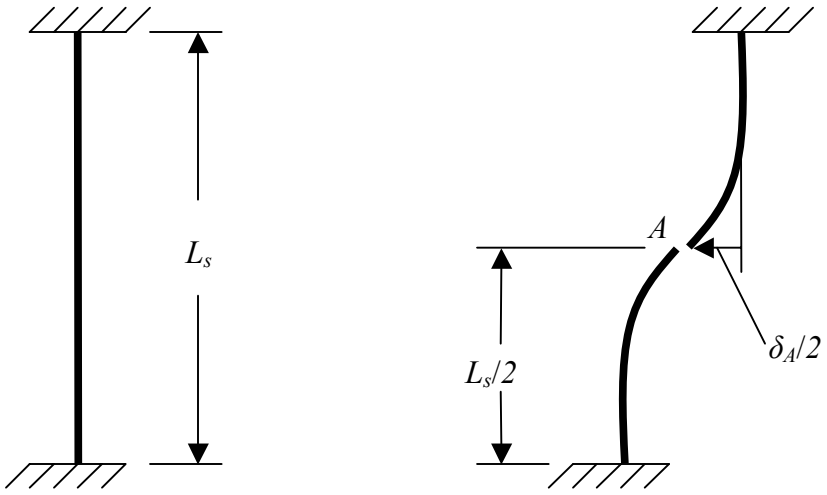

a) b)

Figure 8 Spring Steel Strip a) undeformed, b) deformed

The elastic modulus of steel is 200 GPa and the moment of inertia of the cross section is given by

$$I = \frac{bh^3}{12} \tag{68}$$

where b and h are the width and height of the cross section, respectively. If we choose a force of 1 N for P, we know that a spring with a spring constant of 32.78 N/m should deflect approximately 30.5 mm. Therefore, if P = 1 N, δ_A should be equal to 30.5 mm. As shown in Figure 8b, if the entire strip is to have a deflection of 30.5 mm, then each of the two halves must deflect half that distance, or 15.25 mm.

By substituting the known values into Equation 67, we get the following relation among L_s, b, and h.

$$\delta = 0.01525m = \frac{(1N)(L_s/2)^3}{3(200x10^9\ N/m^2)\left(bh^3/12\right)} \Rightarrow \frac{L_s^3}{bh^3} = 6.1x10^9 \tag{69}$$

Since we only have one equation and three variables, we must choose two of the parameters and then solve for the other one. After some trial and error, values of b = 0.0762 m = 3 in. and h = 0.5 mm were chosen, which give a length of L_s = 0.3873 m = 15.25 in. Therefore, four strips of spring steel with these dimensions collectively have the same effect on the large mass as a spring with a spring constant of 131.1 N/m.

As stated above, the pendulum effect acts against displacement as does the deflection of the strips, but now that we have values for the dimensions of the strips, we can attempt to quantify this effect. Figure 9 shows an illustration of the pendulum effect where x is the lateral displacement of the object and Δ is the resultant vertical displacement. We can write the following two equations for the two unknowns α and Δ.

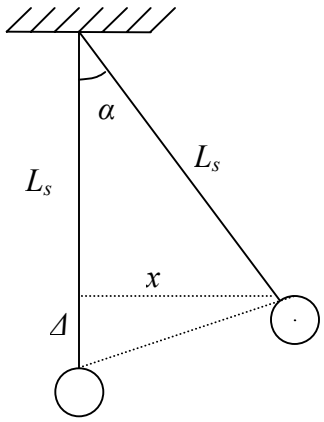

Figure 9 Pendulum Effect Illustration

From simple trigonometry, we have

$$\sin\alpha = \frac{x}{L_s} \Rightarrow \alpha = \sin^{-1}\frac{x}{L_s} \qquad 70)$$

and

$$\cos\alpha = \frac{L_s - \Delta}{L_s} \Rightarrow \Delta = L_s(1-\cos\alpha)\,. \qquad 71)$$

From Figure 6, we can see that the maximum lateral deflection of the large mass at any time is approximately 8 mm. Therefore, if we substitute x = 8 mm and L_s = 0.3873 m into Equations 70 and 71 we get values of α = 1.184˚ and Δ = 0.008 mm. This vertical displacement of 0.008 mm is small compared to the lateral deflection (0.1% of the lateral deflection) but preliminary calculations showed that the pendulum effect may, in fact, tend to act against the displacement of the mass with a greater force than the strips of spring steel. If later experimentation shows that this pendulum effect has a large influence on the operation of the system, then it may be desirable to redesign the suspension system to eliminate the effect (See Section 5.2).

CHAPTER 3

NEW MOTION SYSTEM CONSTRUCTION

3.1 System Fabrication

In order to implement the designs discussed in the preceding chapters, various mechanical parts and structures had to be designed and fabricated. (Drawings of all the parts that were manufactured for this project can be seen in Appendix B.) Two of these parts have already been briefly discussed: the new valve used in conjunction with the solenoid valve and the strips of spring steel. In addition to these elements, a structure from which to suspend the large mass, a housing and rod for each of the cylinders, air supply needles, and the new valve casing were also designed.

3.1.1 Steel Rack and Bucket

Figure 10 below shows a picture of the rack that was designed to suspend the large mass, or bucket. This was manufactured entirely out of steel by Southern Perfection Fabrication in Byron, GA. The bucket design was chosen in order to avoid having to try to hold up 100 lbs and bolt it to the strips of spring steel. With the bucket initially empty, the assembly process was much easier and more mass was added after the bucket was suspended. Also, this design offered the possibility of changing the system parameters if necessary by adding or removing mass from the bucket.

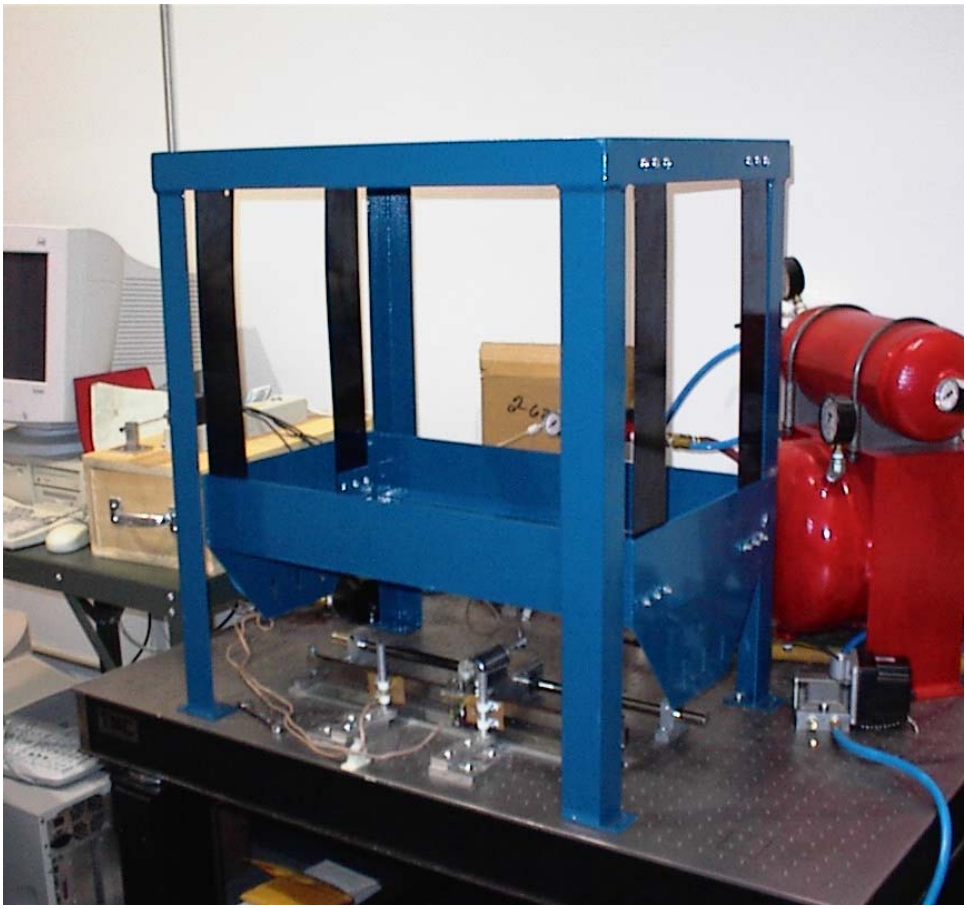

Figure 10 Steel Rack and Bucket

In order to ensure that the pneumatic cylinders would line up exactly with the center of gravity of the scanner head, the rack and bucket had to be designed to allow for subtle adjustment in the vertical direction and in the horizontal direction both parallel and perpendicular to the scanning motion. In order to achieve the vertical adjustment, the part that affixes the cylinders to the bucket ("Bucketpiece" p. 62 Appendix B) mates with slotted holes in the bucket. Therefore, this piece can be moved up and down before being bolted in place to ensure that the cylinders are placed properly. Similarly, the legs of the rack have slotted holes so that the rack can be adjusted in a horizontal direction

perpendicular to the scanning motion when it is mounted to the optical table. The horizontal adjustment parallel to the scanning motion is achieved through the use of the threaded rods which connect the cylinder housings to the bucket.

3.1.2 Cylinder Housings

A picture of the special cylinder housings that were designed is shown in Figure 11. The purpose of these housings is to protect the delicate glass structure of the cylinders while providing a way to rigidly attach the cylinders to the bucket. Each of the housings consists of two pieces which are screwed together in the middle and enclose the

Figure 11 Cylinder Housing

entire cylinder. These two parts are named "Case 1" and "Case 2" and drawings of them can be seen on pages 63 and 64 of Appendix B. The three threaded rods are used to attach each of the housings to the bucket. As shown in Figure 11, the outside of each half of the housing has three holes which the threaded rods pass through. Then, nuts are screwed onto each end of the rods to fix the housing in place.

Another purpose of these housings is to create part of the precharge volume. Figure 12 below shows a hidden-line view of the front half of the housing, or "Case 2". From this drawing, it can be seen that there is an open volume between the front of the cylinder and the inside surface of the part. There is a hole that connects this volume to the outside of the part. This is, in fact, where the new valve structure is attached to the housing and the hole leads directly to the cavity discussed in Section 2.2.3. Therefore, this open volume in front of the cylinder is part of the precharge volume along with the cavity and the volumes leading to and from the cavity. In the figure, the precharge volume is shaded in gray. The volume inside the connector leading from the bottom of the cavity to the miniature solenoid valve is also included in the precharge volume even though this connector is not shown in Figure 12.

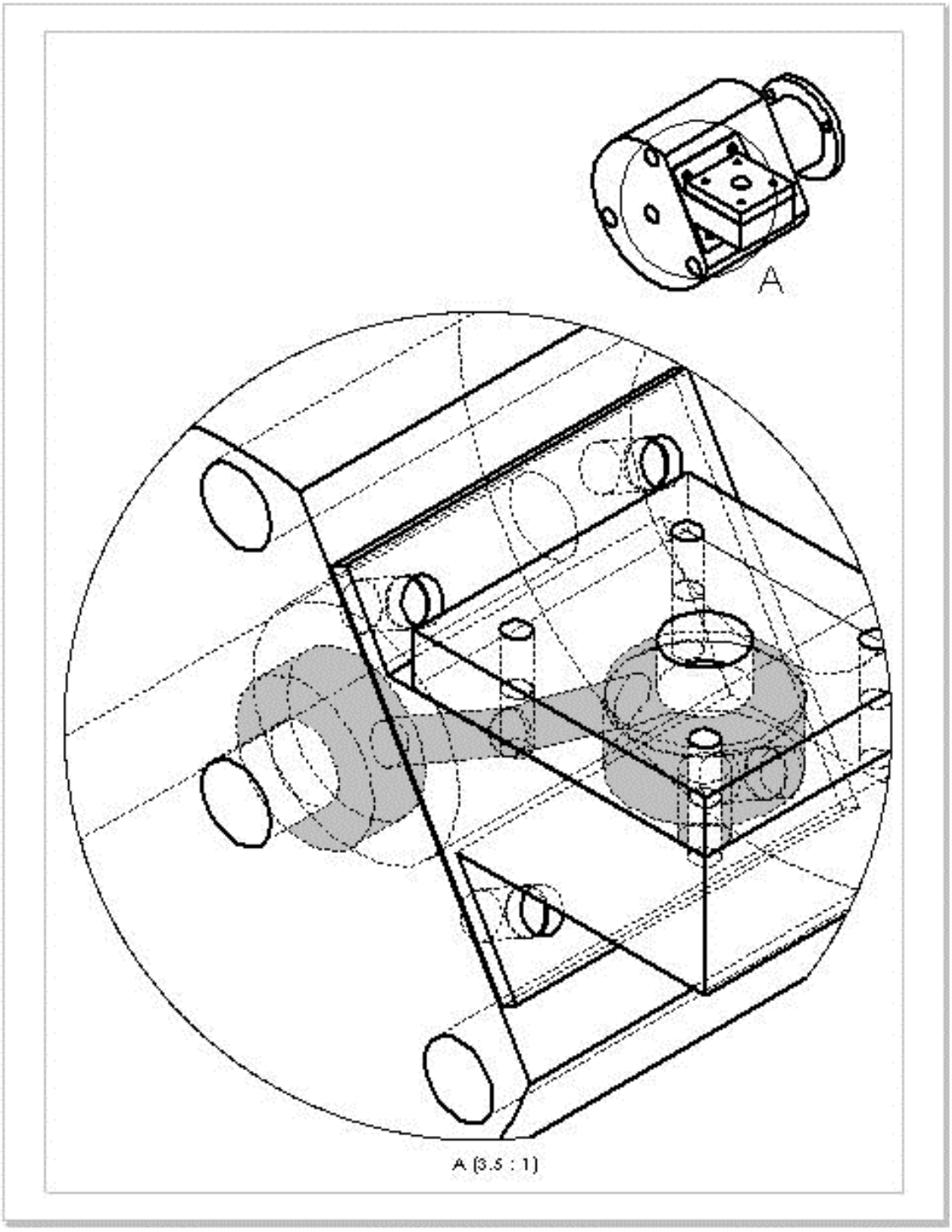

Figure 12 Hidden-Line View of Case 2

3.1.3 Cylinder Rods

The main design consideration with the rods was buckling. We chose to make the rods out of aluminum and we wanted to make sure that the safety factor against buckling was sufficient. If the rod is in the Euler region of buckling, then the diameter is given by the equation

$$d_r = \left(\frac{64 F_p L_e^2}{\pi^3 E_{Al}} \right)^{1/4} \qquad 72)$$

where L_e is the equivalent length (twice the actual length in this case), F_p is the piston force, and E_{Al} is the elastic modulus of aluminum. From Table 1, the largest supply pressure is 76.1 psig. At this pressure, the piston force is 103.9 N. If we want to determine the necessary diameter to have a safety factor of 4, then we use a value of 4 times 103.9 N, or F_p = 415.6 N. The length of the rod will be the stroke of the cylinder (100 mm). The elastic modulus of aluminum is 71 GPa. Therefore, the necessary diameter for a safety factor of 4 from Equation 72 is 4.69 mm. We used a rod with a diameter of 0.25 in. = 6.35 mm, so the safety factor is even greater than 4. A simple calculation of the slenderness ratio with this length and diameter showed that the assumption that the rod was in the Euler region of buckling was valid. A drawing of the rods can be seen on page 71 in Appendix B.

3.1.4 Valve Structure

The new valve structure consists of two parts: a lower part that is mounted to the

side of the housing and an upper part that is attached to the top of it. These two parts are called "Valve Bottom" and "Valve Top" and drawings of them can be seen in Appendix B. There are right- and left-handed versions of the valve bottom to be mounted on the two housings, but the valve top is symmetric, so there is only one version of that part. These two parts together form the structure that is described in Figure 4 on page 28. The cavity is machined into the valve bottom. The valve top is screwed on to cover the cavity and the thin disk is enclosed inside. The top is open to the atmosphere as shown in Figure 4 and the bottom is connected to the miniature solenoid valve.

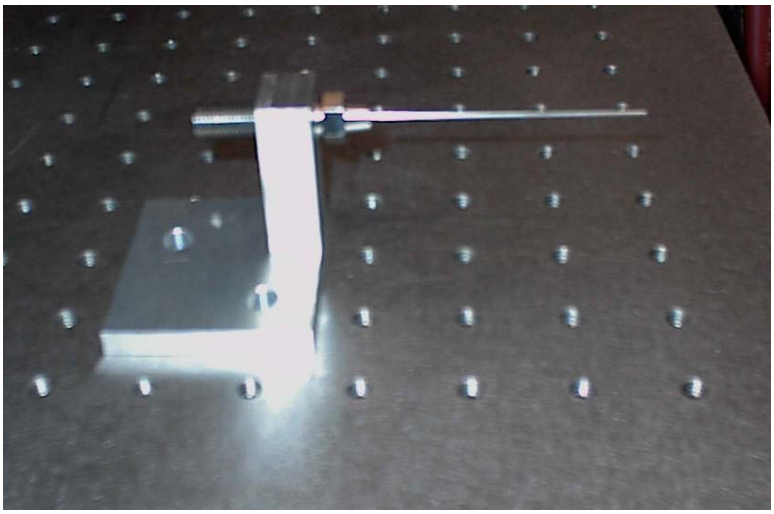

Figure 13 Needle and Needle Mount

The two needles used in the air supply system for the air bearings were modeled directly after blow gun needle nozzles as described in Section 2.1.1. Instead of mounting the needles to the bucket like the cylinders, they were mounted directly to the table. The reason for this is that the needles must engage very precisely with the scanner head. The

bucket only has a very small range of motion during operation, but it does deflect several millimeters. If the needles were mounted to the bucket, they would also be subject to this motion. Trying to precisely engage the scanner head and the needle when both of them are in motion would have been very difficult to design and far more complex than necessary. By mounting the needles to the table, they remain stationary during operation and this complexity is avoided. A picture of one of the needles and the mounting piece is shown in Figure 13. The air flow to the needles is controlled by the same two valves that were used to control the air flow to the cylinders in the previous design. These are Parker CCJ1 Series Valves and they are discussed in Section 3.3.2 of Mr. Butcher's thesis.

CHAPTER 4

CONTROL SCHEME

4.1 Control Algorithm

The system is again controlled using the Motorola MC68HC11E9 (or simply HC11) microcontroller as it was in the previous design; however the control algorithm is slightly different. Once again, two photo interrupters are used to measure the velocity of the scanner head and then the necessary times to actuate the four valves are calculated based on these velocities. The obvious goal of the control scheme is to maintain the desired velocity of the scanner head.

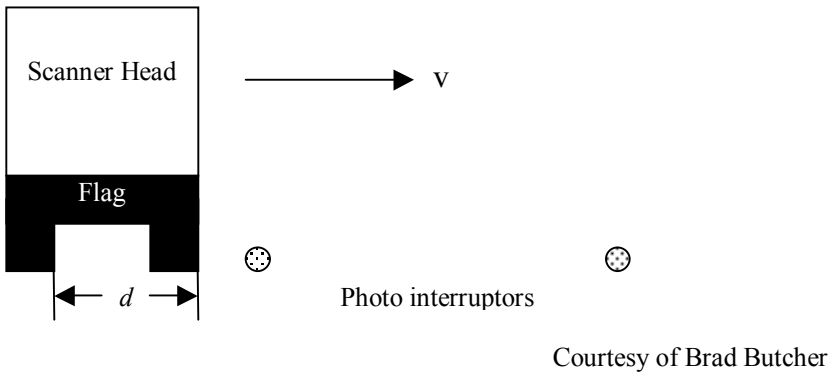

Figure 14 Flag on Scanner Head

Figure 14 shows a drawing of the positions of the photo interrupters and how they are used to measure the scanner head's velocity. There is a flag attached to the scanner head that has two arms which are separated by a known distance, *d*. The HC11 first records the time at which the leading edge of the first arm breaks the first photo

interrupter. At this time, the miniature solenoid valve at the other end (the right end in Figure 14) is opened and the precharging of the small volume on the rod side of the cylinder begins. As the scanner head continues down the track, the leading edge of the second arm breaks the first photo interrupter and the HC11 also records this time. Using these two recorded times, the HC11 calculates the velocity by computing the change in position, *d*, divided by the change in time. It calculates this velocity while the head is traveling between the two photo interrupters.

Based on this velocity it also calculates the time the will elapse between the leading edge of the second arm of the flag breaking the second photo interrupter and the scanner head impacting the rod. This is how the air flow to the needle is turned on and the precharge volume is sealed at the appropriate time. Recall that the system was designed so that the needle would engage with the head at the same time the head impacted the rod. Therefore, by calculating the time at which the head will impact the rod, the HC11 knows when to actuate the valve and open the flow of air to the needle. At this same moment, the miniature solenoid valve is closed and the precharge volume is sealed.

The pressure in the precharge volume is what makes the scanner head velocity converge to the desired velocity. Recall that Equation 46 was used in part to determine the necessary precharge pressure and volume that would be equivalent to replacing the energy lost due to momentum transfer and piston friction when the head was traveling at the desired velocity. By using these same values for the precharge pressure and volume (the precharge volume is fixed anyway, but the precharge pressure can be changed by closing the miniature solenoid valve after a certain amount of time so that only a certain

mass of air is injected into the volume) during every pass of the scanner head, the velocity will naturally converge to the desired velocity.

The reason for this is that the system will reach a steady state where the energy that is lost during each pass will be exactly equal to the energy that is being supplied. Initially, the motion is started by manually opening a valve to one of the cylinders which is connected to the supply pressure. This sets the head in motion at a velocity lower than the desired velocity because the switching time of a manually actuated valve is much longer than that of an electrically actuated valve. Therefore, the head is initially traveling slower than desired, but we are adding the amount of energy that would be lost if it were traveling at the desired velocity. We are actually adding more energy than what is lost, so the velocity on the next pass will increase. In addition, if there is small overshoot when the head approaches the desired velocity, the same effect will tend to decrease the speed since the amount of energy lost will be greater than the supplied energy. This process causes the scanner head to converge to the desired velocity without having to vary the precharge pressure with every pass.

CHAPTER 5

CONTRIBUTIONS OF THESIS AND FURTHER WORK

5.1 Completion of Objectives

The three main goals of this project involved implementing a mode of tetherless operation of the scanner, designing an alternative method of energy replacement, and isolating the vibration of the table which was occurring at higher velocities. The tetherless operation was achieved by designing an air supply system utilizing blow-gun-type needle nozzles. These special needle nozzles engage with the scanner head at each end of the track while the head is in contact with the rods. They supply a certain amount of air to the scanner head to maintain the tank pressure at or above 60 psig which is the required pressure for the air bearings to operate correctly. The appropriate length and diameter of the needles were calculated to ensure that the mass flow rate would be sufficient to actually maintain this tank pressure.

In order to find a better way of adding energy to the system, the two main energy losses, momentum transfer and piston friction, were quantified and a method of precharging a certain volume of air on the rod side of each cylinder was devised. When the scanner head impacts the rod the volume on the rod side increases, the pressure decreases, and a certain amount of work is done. This pressure and volume were selected such that the amount of work done in the expansion process is equal to the energy losses due to momentum transfer and piston friction. Two miniature solenoid valves from The Lee Company were purchased to inject the air into the precharge volumes. In addition to

this, a new valve was designed to allow the volume to be opened to the atmosphere when the expansion process causes it to reach atmospheric pressure and to remain open while the piston forces the head in the opposite direction.

The table vibrations were isolated by designing a structure featuring a large, suspended, inertial mass. This mass hangs from four strips of spring steel which function as linear springs by returning the mass to a neutral position when it is deflected. The cylinders are mounted to this large mass instead of the optical table which they were mounted to in the previous design. During operation of the scanner, the repeated impacts of the scanner head and the rods cause the large mass to swing back and forth several millimeters, but the only force that gets transmitted to the table is the small spring force caused by this small deflection. As shown in Figure 7, this force is roughly 100 times less than in the previous design where that entire piston force was transmitted to the table. Overall, this project showed how the previous design could be modified to meet higher performance specifications and it reinforced the concept of a linear motion system driven by pneumatic pistons.

5.2 Further Work

The next step in this project is experimentation with the new system in order to verify the theoretical calculations and assertions put forth in this paper. Possible areas of experimentation include the operation of the new valves that control the air flow to and from the precharge volumes, and the functioning of the new low-friction cylinders along with the cylinder housings that were designed. Regarding the new valves, work must be

done to ensure that the valves open and close fast enough and at the appropriate times to allow proper air flow to the precharge volumes. This will be critical since the function of the air in the precharge volume is to supply energy to the system. Work must also be done to make sure that the low-friction cylinders that were purchased will function well inside the housings that were designed and fabricated for this project.

Some possible amendments to this design could include a redesign of the way that the large inertial mass is suspended and replacement of the needles as a method of supplying air to the air bearings. The large mass could be suspended by a structure that functioned solely using the pendulum effect as a spring. Figure 15 shows a possible structure of cables that would effectively be a pendulum with the large suspended mass on the end. This would eliminate the actual spring from the design and make the suspension structure the only thing that returned the large mass back to the neutral position.

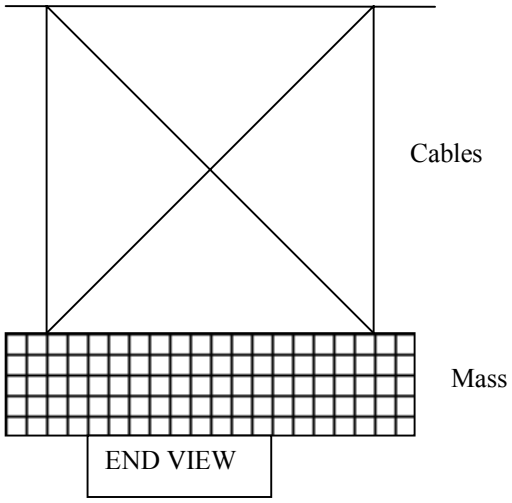

Figure 15 New Suspension System

If the needles proved not to be a feasible method of providing air to the air bearings, they could possibly be replaced by a piston pump on the scanner head itself. Figure 16 shows a drawing of a piston pump on the traveling head.

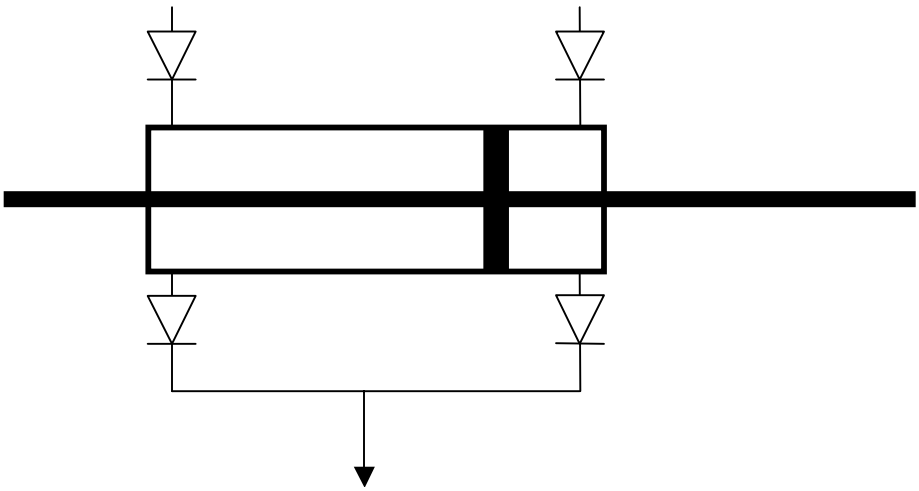

Figure 16 Piston Pump on Traveling Head

This setup would also have the advantage of reducing the impact forces on the traveling head and thereby reducing the energy lost to momentum transfer between the head and the piston/rod.

APPENDIX A

MATLAB CODE

```
% Author: Matt Boyd

% Date: April 10, 2003

% This function plots the position and velocity of the scanner head and
% the large suspended mass given the system parameters.  It also plots
% the force exerted on the grounded unit by the suspended mass.

function scannermodel3(a, v, F, M1, M2, B2, k)

% 'a' is the length 'delta_desired' in meters.
% 'v' is the desired velocity in m/s.
% 'F' is the force exerted by the piston in Newtons.
% 'M1' is the mass of the scanner head in kg.
% 'M2' is the mass of the suspended mass in kg.
% 'B2' is the damping constant in Ns/m.
% 'k' is the spring constant in N/m.
b=a+0.46; % 'a' + track length of 46 cm
c=a+b;

% System model with states q1=position of scanner head, q2=position of
% suspended mass, q3=velocity of scanner head, q4=velocity of suspended
% mass.
A=[0 0 1 0; 0 0 0 1; 0 0 0 0; 0 -k/M2 0 -B2/M2];
B=[0 0 1/M1 -1/M2]';

% Discretize the system using a sampling time of 1 ms.
T=0.001;
[G, H]=C2D(A, B, T);

% Initialize matrices.
q1=[]; q2=[]; q3=[]; q4=[];

% Loop to calculate the states at each time step.
for i=1:20000; q1(1)=0; q2(1)=0; q3(1)=0; q4(1)=0;
    % For positive scanner head velocity
    if q3(i)>=0;
        % While head is in contact with the left cylinder
        if (q1(i)-q2(i))<=a-v*T;
              u(i)=F;
        % While head is in contact with the right cylinder
        else if (q1(i)-q2(i))>=b-v*T;
                u(i)=-F;
        % While head is not in contact with either cylinder
        else
            u(i)=0;
            if q3(i)<v;
                % This adds a little energy to both sides to make up
                % for the energy taken out by the damper.
                q3(i)=v;
                q4(i)=-v*(M1/M2);
            end %if
        end %else if
        end %if
    end %if
    % For negative scanner head velocity
    if q3(i)<0;
```

```
        % While head is in contact with the left cylinder
        if (q1(i)-q2(i))<=a+v*T;
            u(i)=F;
        % While head is in contact with the right cylinder
        else if (q1(i)-q2(i))>=b+v*T;
                u(i)=-F;
        % While head is not in contact with either cylinder
        else
            u(i)=0;
            if q3(i)>-v;
                % This adds a little energy to both sides to make up
                % for the energy taken out by the damper.
                q3(i)=-v;
                q4(i)=v*(M1/M2);
            end %if
        end %else if
        end %if
    end %if

% Discrete-time system model
q1(i+1)=G(1,1)*q1(i)+G(1,2)*q2(i)+G(1,3)*q3(i)+G(1,4)*q4(i)+H(1)*u(i);
q2(i+1)=G(2,1)*q1(i)+G(2,2)*q2(i)+G(2,3)*q3(i)+G(2,4)*q4(i)+H(2)*u(i);
q3(i+1)=G(3,1)*q1(i)+G(3,2)*q2(i)+G(3,3)*q3(i)+G(3,4)*q4(i)+H(3)*u(i);
q4(i+1)=G(4,1)*q1(i)+G(4,2)*q2(i)+G(4,3)*q3(i)+G(4,4)*q4(i)+H(4)*u(i);

end %for

% Plot the positions, velocities, and force exerted on the grounded
unit.
x=[0:20000];
subplot (2, 2, 1); plot(x, q1)
ylabel('position of x1 (m)')
xlabel('time (ms)')
subplot (2, 2, 2); plot(x, q2)
ylabel('position of x2 (m)')
xlabel('time (ms)')
subplot (2, 2, 3); plot(x, q3)
ylabel('velocity of x1 (m/s)')
xlabel('time (ms)')
subplot (2, 2, 4); plot(x, q4)
ylabel('velocity of x2 (m/s)')
xlabel('time (ms)')
figure(2);
plot(x, k*q2+B2*q4)
ylabel('Force exerted on table (N)')
xlabel('time (ms)')
```

APPENDIX B

DRAWINGS

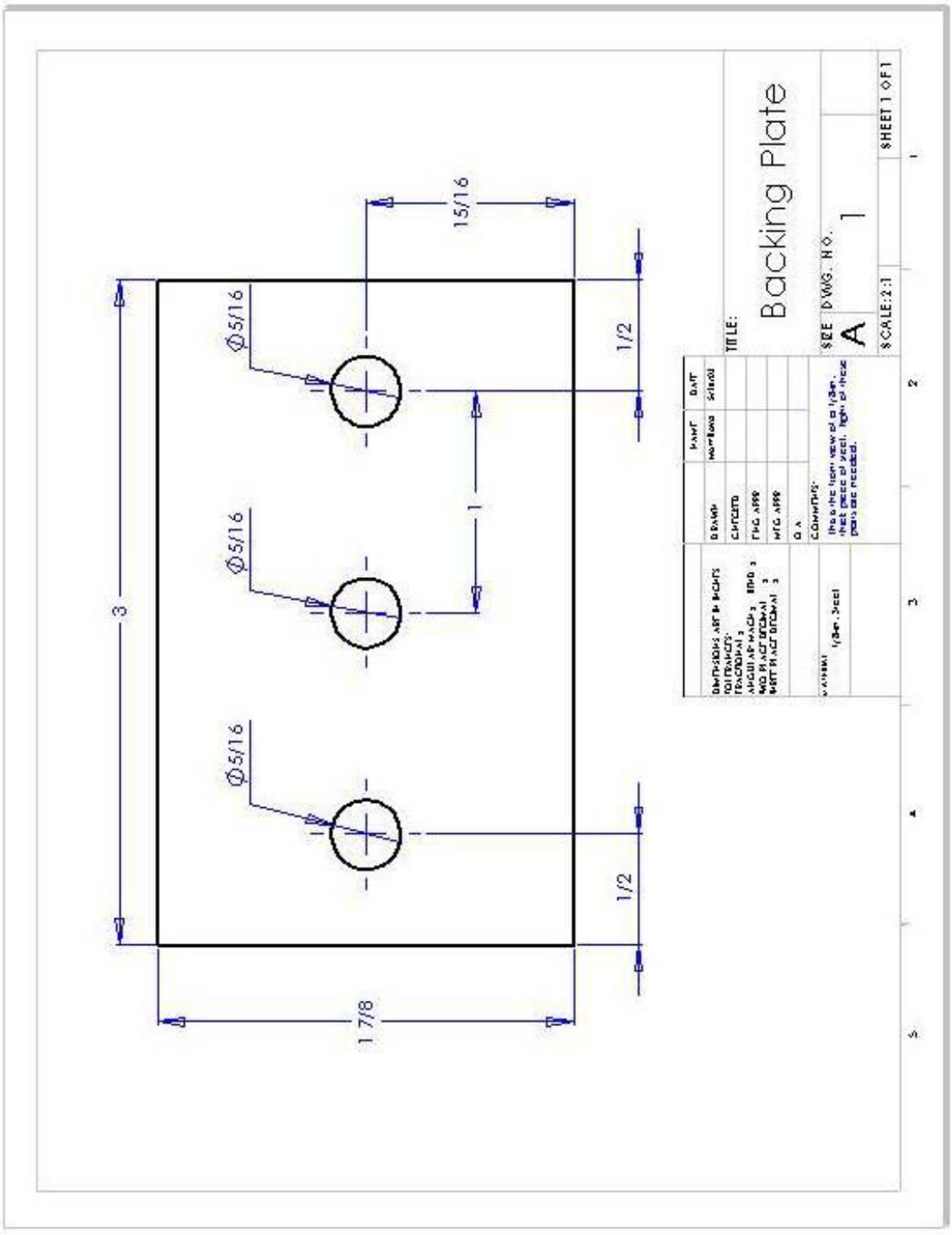
Ø5/16
Ø5/16
Ø5/16
15/16
3
1
1/2
1/2
1 7/8
Backing Plate
A
1
SCALE:2:1
SHEET 1 OF 1

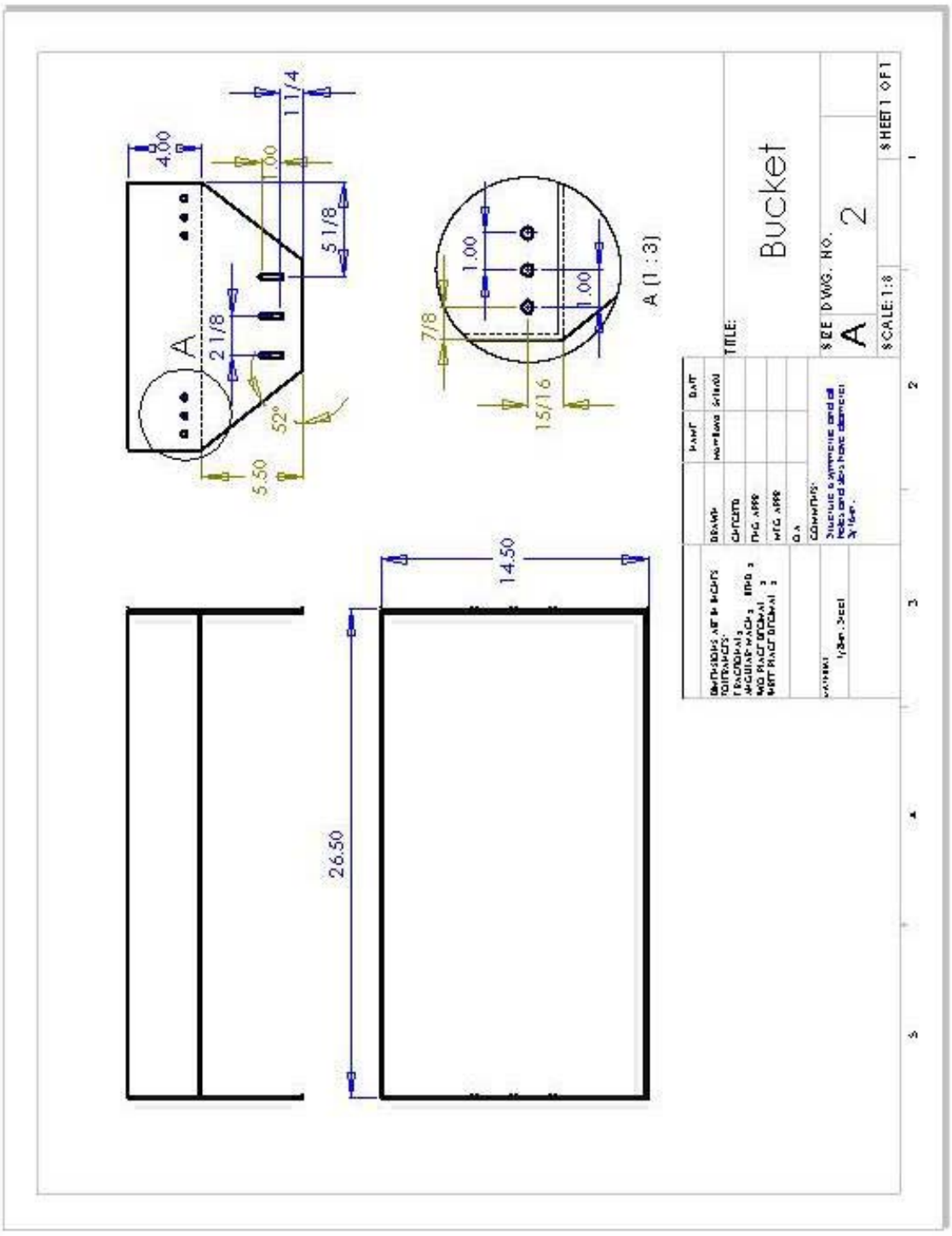
Bucket
A
A (1 : 3)
4.00
1.00
1 1/4
5 1/8
2 1/8
52°
5.50
7/8
1.00
1.00
15/16
14.50
26.50
TITLE:
SIZE
A
DWG. NO.
2
SCALE: 1:8
SHEET 1 OF 1

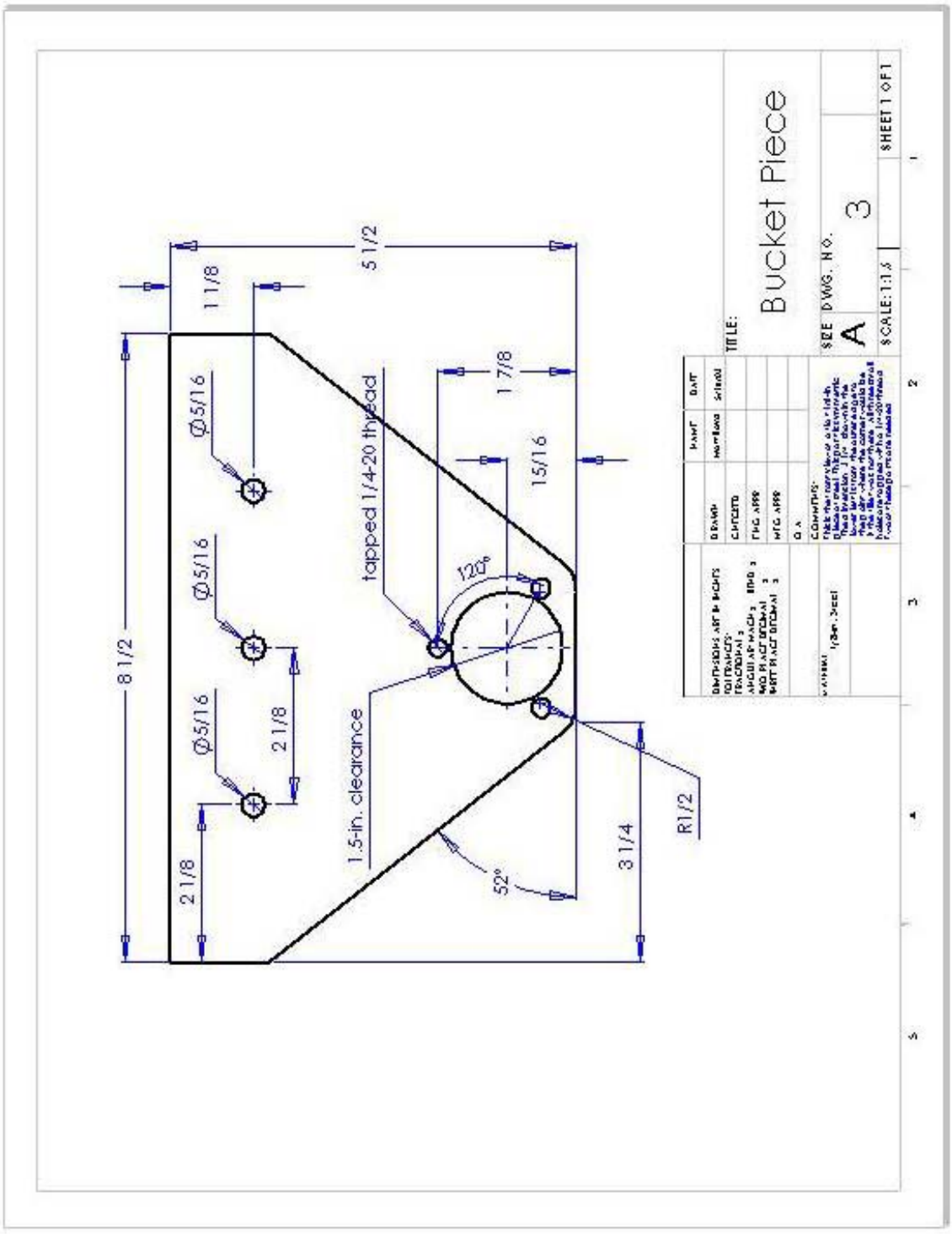
8 1/2
2 1/8
Ø5/16
Ø5/16
Ø5/16
2 1/8
1.5-in. clearance
tapped 1/4-20 thread
1 1/8
5 1/2
1 7/8
15/16
120°
52°
3 1/4
R1/2
Bucket Piece
A
3

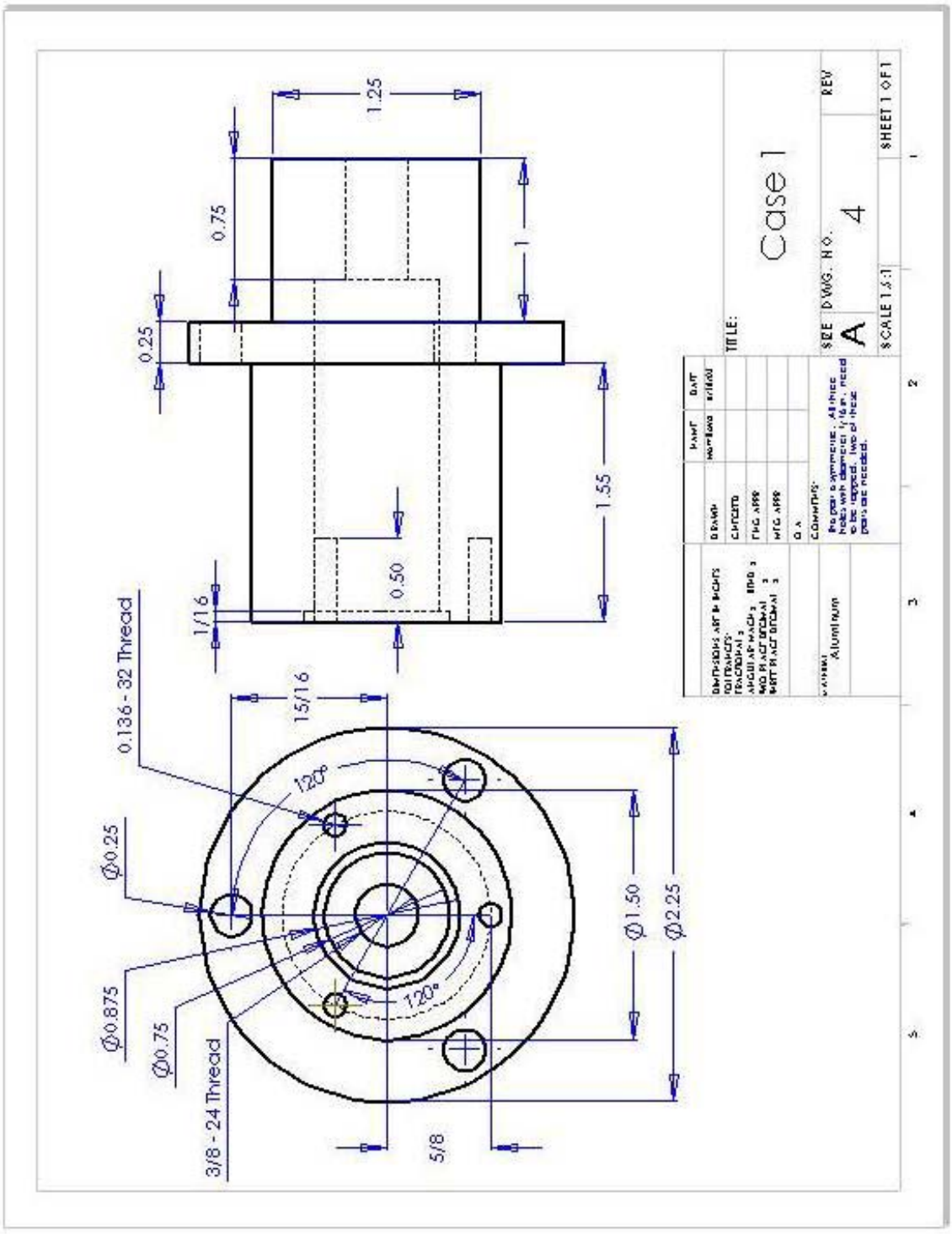
1.25
0.75
1
0.25
1.55
0.50
1/16
0.136 - 32 Thread
15/16
120°
Ø0.25
Ø0.875
Ø0.75
3/8 - 24 Thread
Ø1.50
Ø2.25
5/8
Case1
TITLE:
SIZE
A
DWG. NO.
4
REV
SCALE 1.5:1
SHEET 1 OF 1

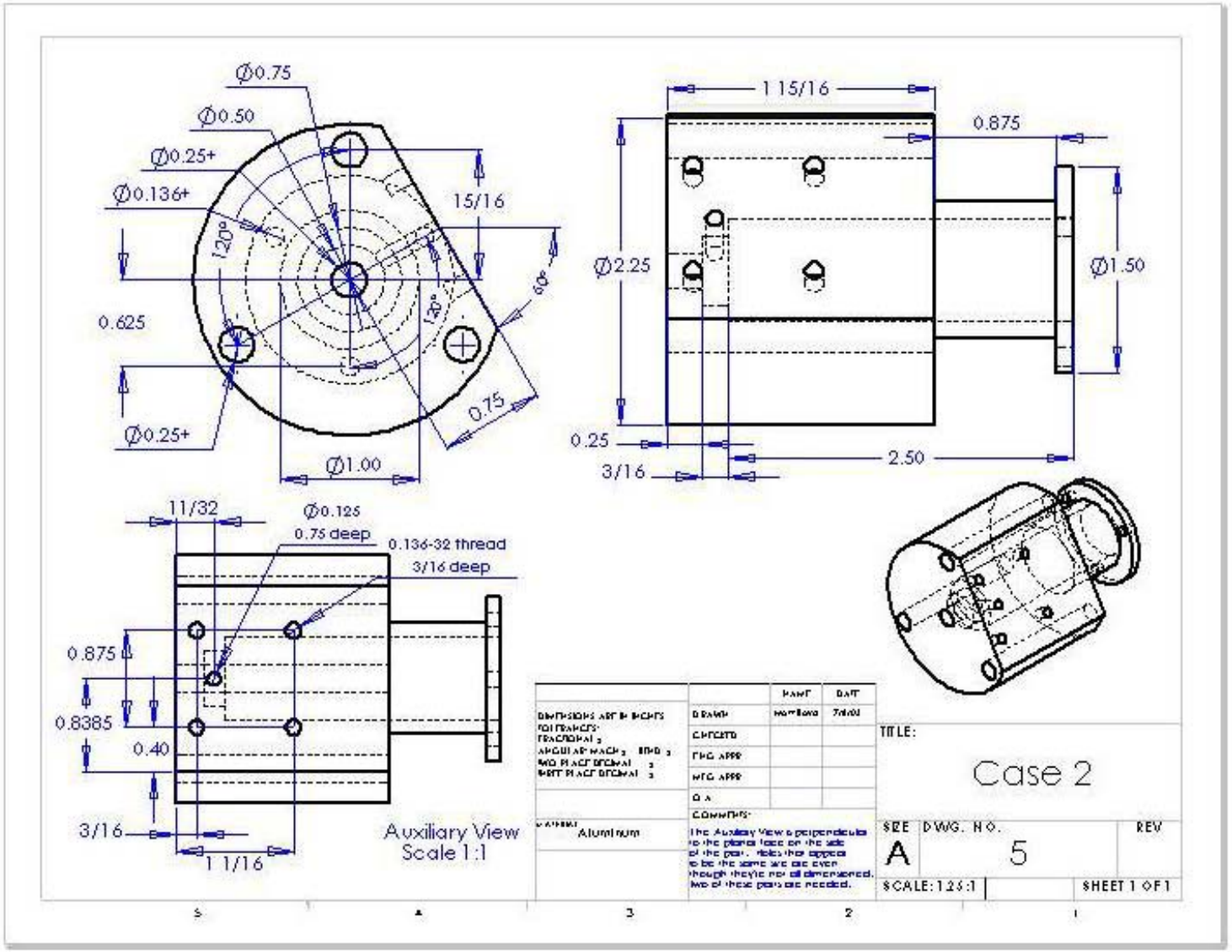
Ø0.75
Ø0.50
Ø0.25+
Ø0.136+
120°
15/16
60°
0.625
Ø0.25+
0.75
Ø1.00
1 15/16
0.875
Ø2.25
Ø1.50
0.25
3/16
2.50
11/32
Ø0.125
0.75 deep
0.136-32 thread
3/16 deep
0.875
0.8385
0.40
3/16
1 1/16
Auxiliary View
Scale 1:1
Aluminum
Case 2
SIZE
A
DWG. NO.
5
REV
SCALE: 1.25:1
SHEET 1 OF 1

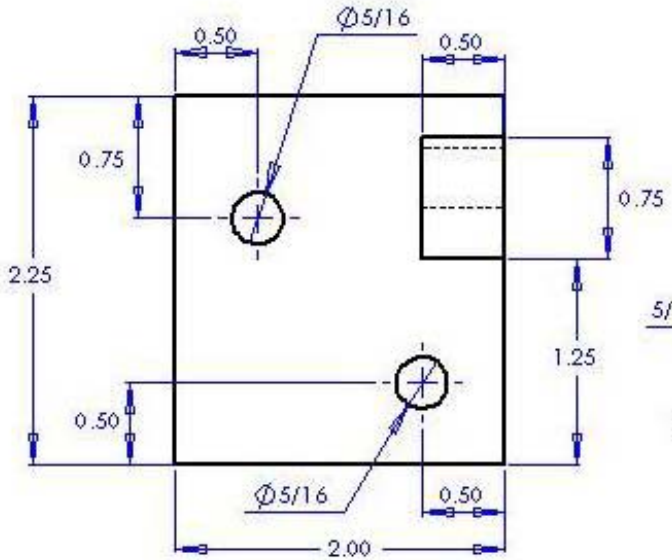

TOP VIEW

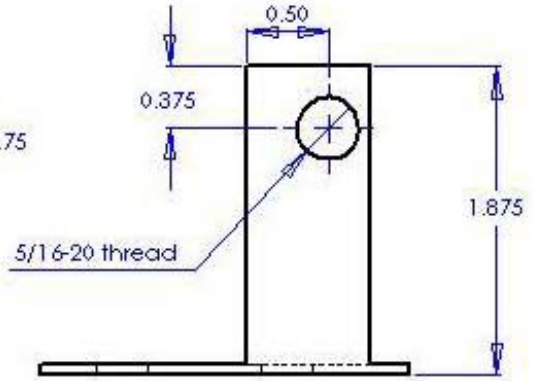

RIGHT SIDE VIEW

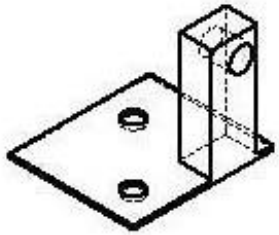

		NAME	DATE
DIMENSIONS ARE IN INCHES TOLERANCES: FRACTIONAL ± ANGULAR: MACH ± BEND ± TWO PLACE DECIMAL ± THREE PLACE DECIMAL ±	DRAWN	[illegible]	7/16/01
	CHECKED		
	ENG APPR		
	MFG APPR		
	Q.A.		
	COMMENTS:		
MATERIAL Aluminum			

TITLE:
Left Needle Mount

SIZE	DWG. NO.	REV
A	6	

SCALE: 1.25:1 | SHEET 1 OF 1

5 4 3 2 1

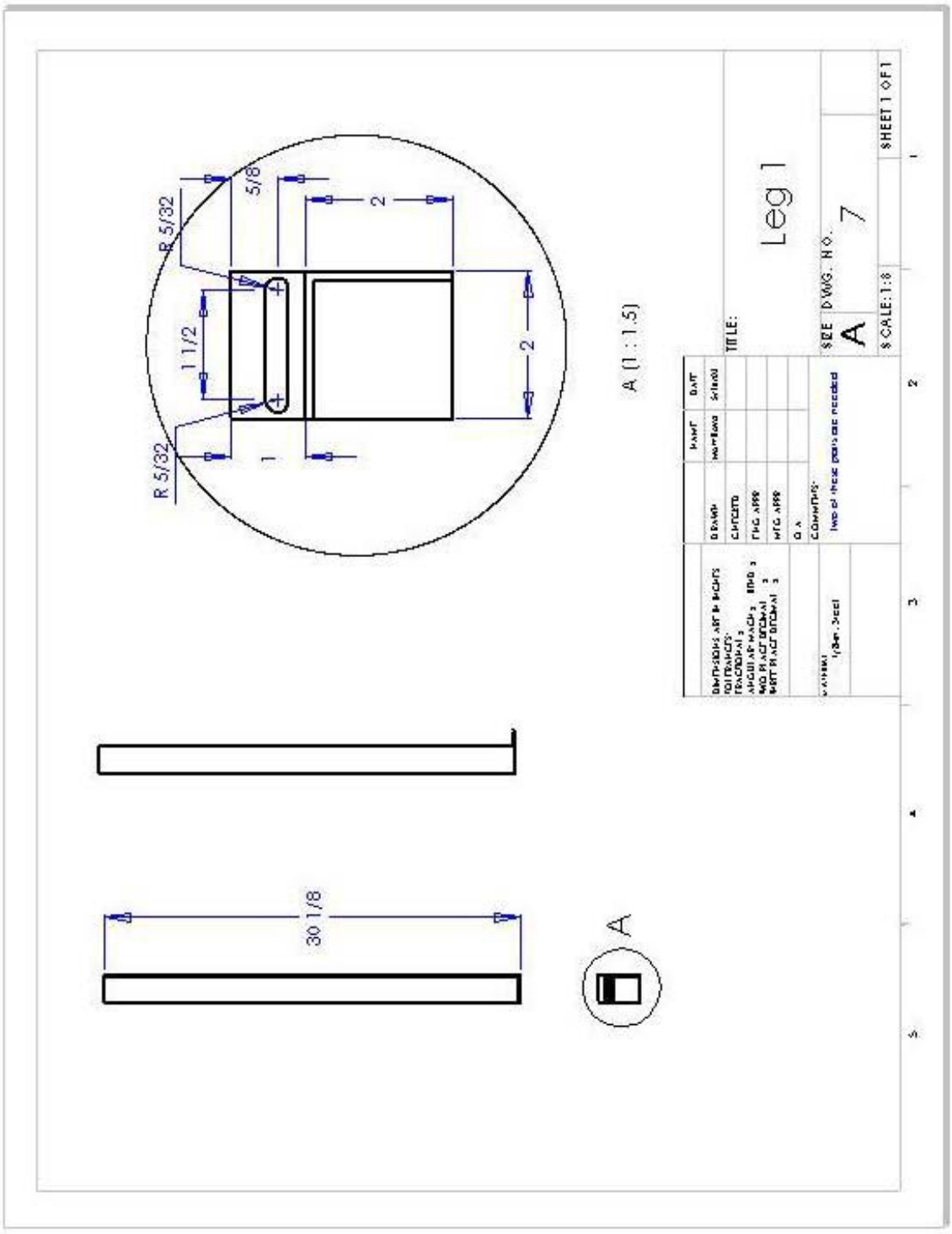
R 5/32
5/8
2
1 1/2
2
R 5/32
1
A (1 : 1.5)
30 1/8
A
TITLE:
Leg 1
SIZE
A
DWG. NO.
7
SCALE: 1:8
SHEET 1 OF 1

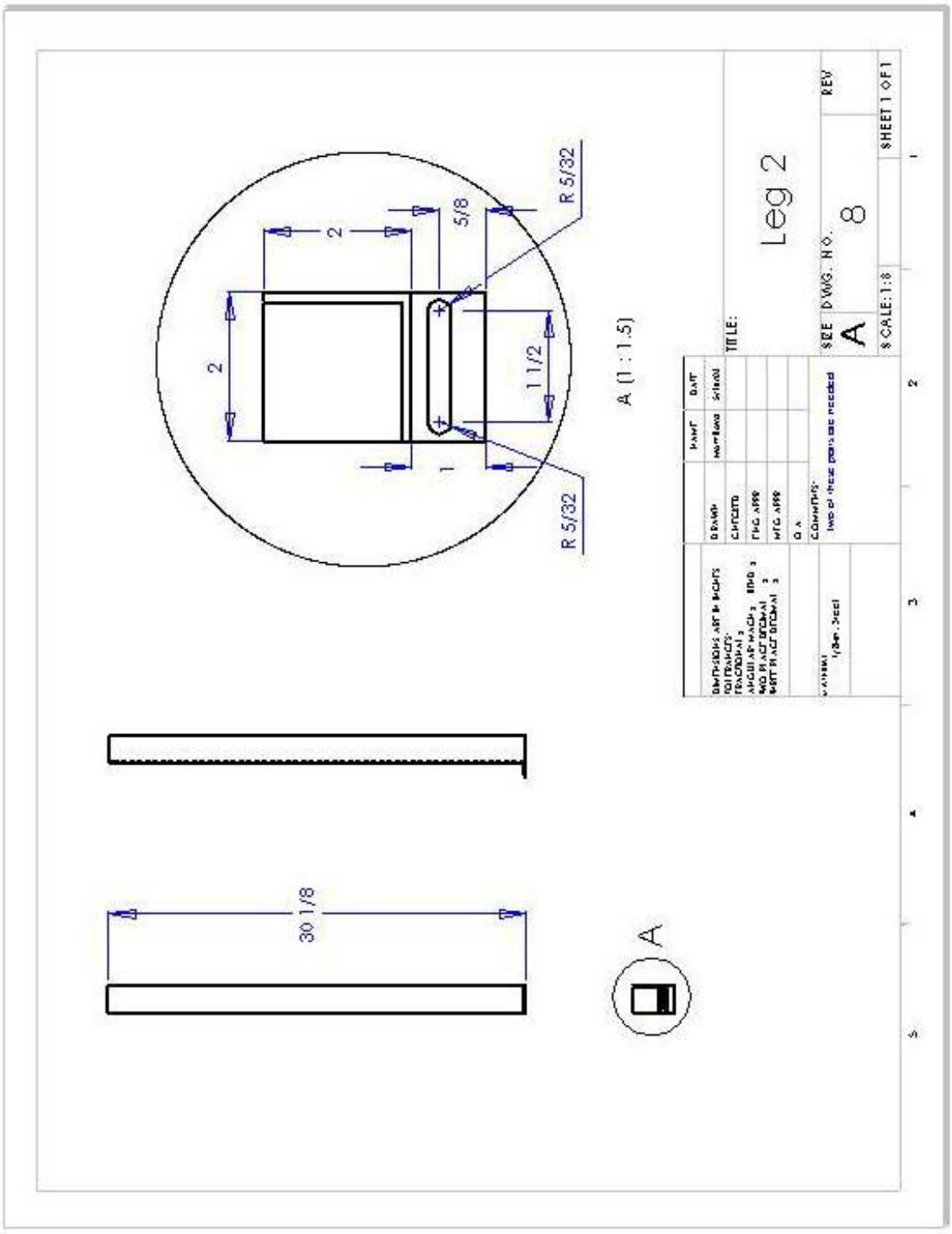
30 1/8
A
A (1 : 1.5)
2
2
5/8
R 5/32
1 1/2
1
R 5/32
TITLE:
Leg 2
SIZE
A
DWG. NO.
8
REV
SCALE: 1:8
SHEET 1 OF 1

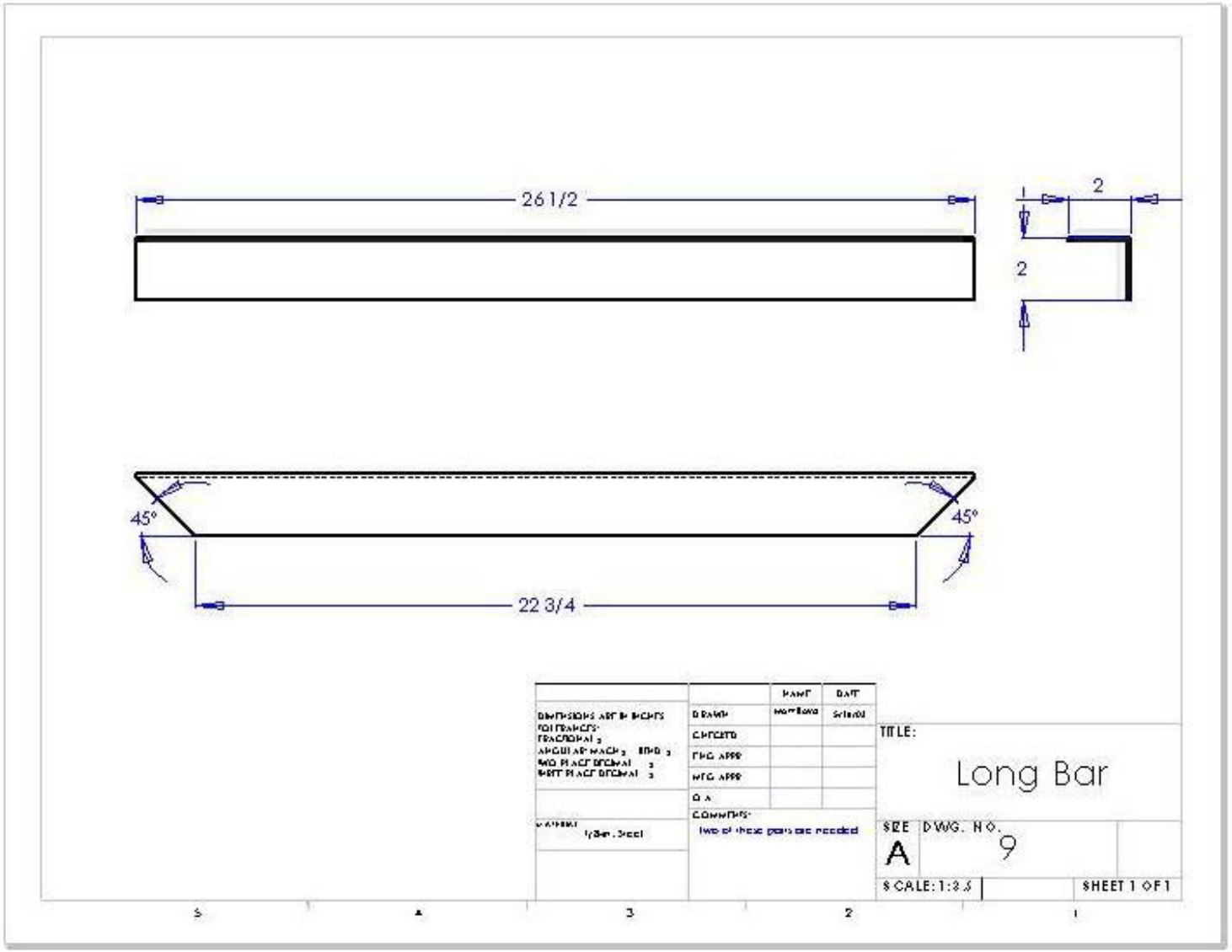
26 1/2
2
2
45°
45°
22 3/4
NAME
DATE
DRAWN
CHECKED
ENG APPR
MFG APPR
Q.A
COMMENTS:
Two of these parts are needed
TITLE:
Long Bar
SIZE
A
DWG. NO.
9
SCALE: 1:2.5
SHEET 1 OF 1

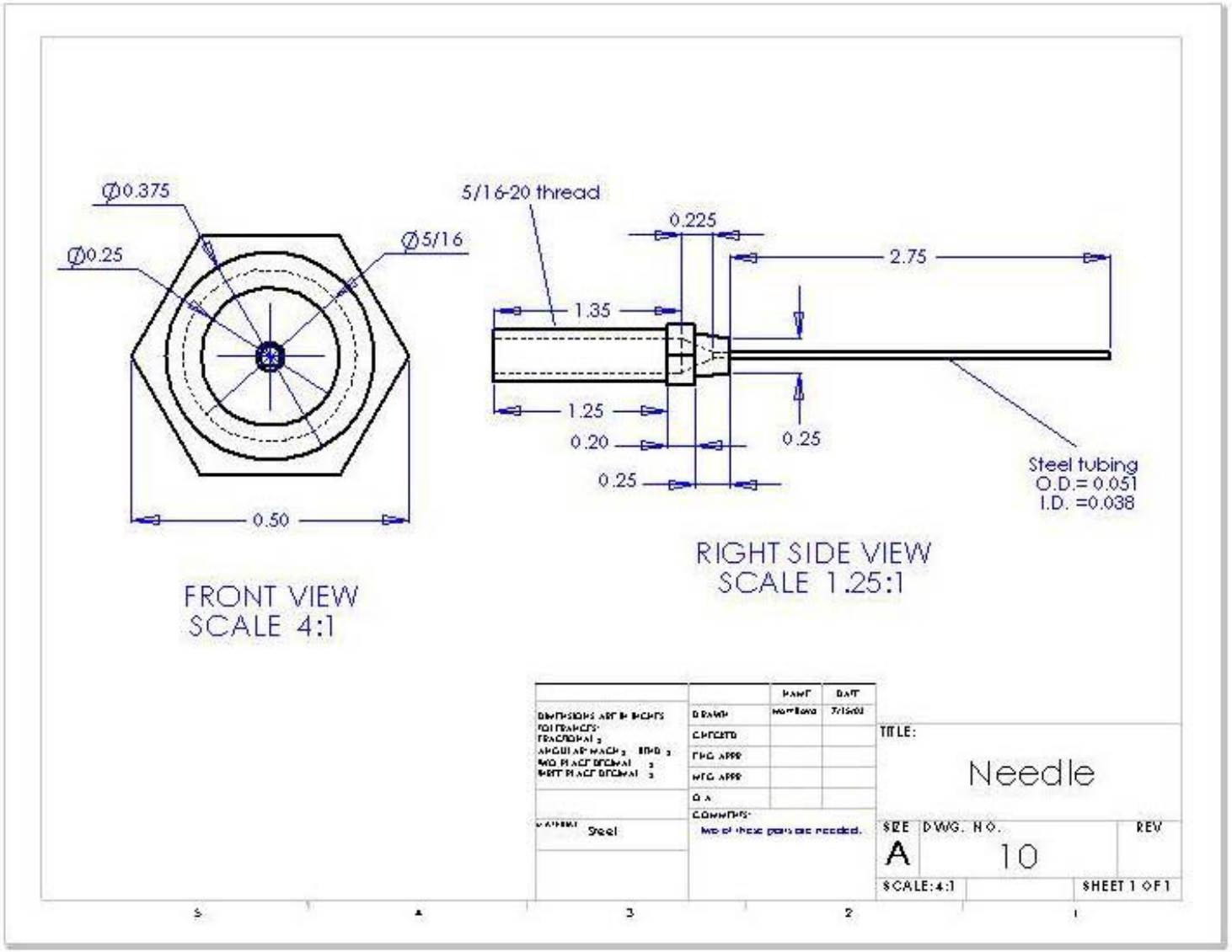
Ø0.375
Ø0.25
Ø5/16
0.50
FRONT VIEW
SCALE 4:1
5/16-20 thread
0.225
2.75
1.35
1.25
0.20
0.25
0.25
Steel tubing
O.D.= 0.051
I.D. =0.038
RIGHT SIDE VIEW
SCALE 1.25:1
NAME
DATE
DRAWN
CHECKED
ENG APPR
MFG APPR
Q.A
COMMENTS:
Steel
TITLE:
Needle
SIZE
A
DWG. NO.
10
REV
SCALE: 4:1
SHEET 1 OF 1

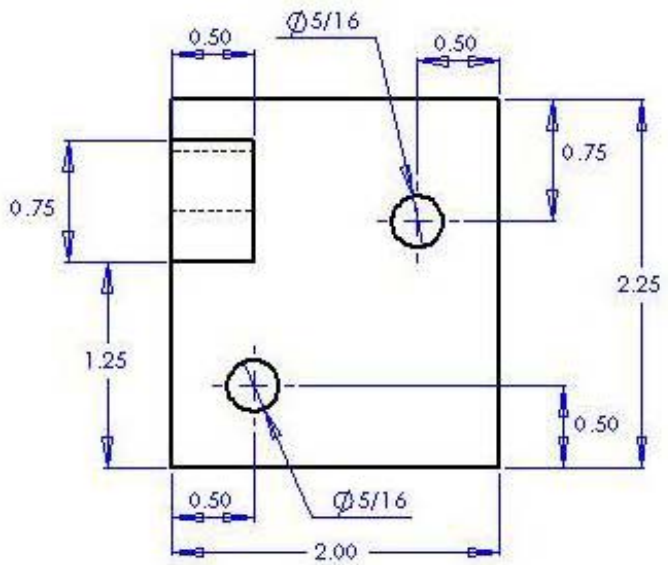

TOP VIEW

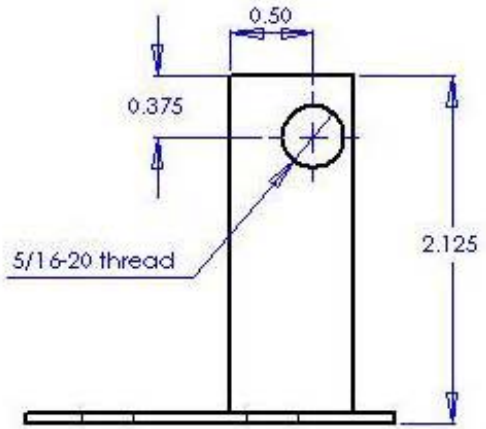

RIGHT SIDE VIEW

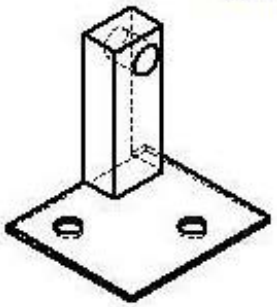

		NAME	DATE
DIMENSIONS ARE IN INCHES TOLERANCES: FRACTIONAL ± ANGULAR: MACH ± BEND ± TWO PLACE DECIMAL ± THREE PLACE DECIMAL ±	DRAWN	Matt Bond	7/16/03
	CHECKED		
	ENG APPR		
	MFG APPR		
	Q.A.		
	COMMENTS:		
MATERIAL: Aluminum			

TITLE: Right Needle Mount

SIZE	DWG. NO.	REV
A	11	

SCALE: 1.25:1 | SHEET 1 OF 1

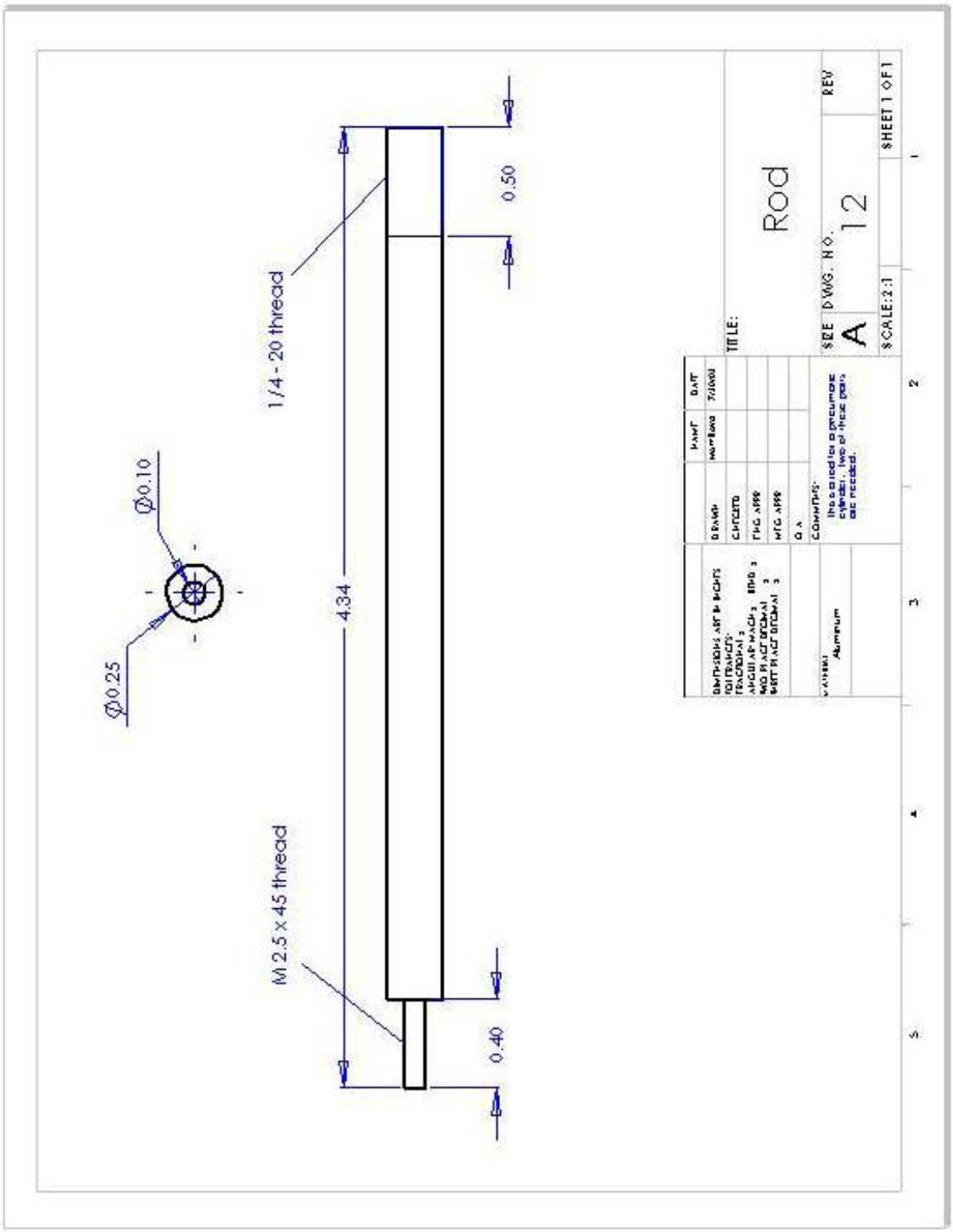
Ø0.10
Ø0.25
1/4 - 20 thread
M 2.5 x 45 thread
4.34
0.50
0.40
TITLE:
Rod
SIZE
A
DWG. NO.
12
REV
SCALE: 2:1
SHEET 1 OF 1

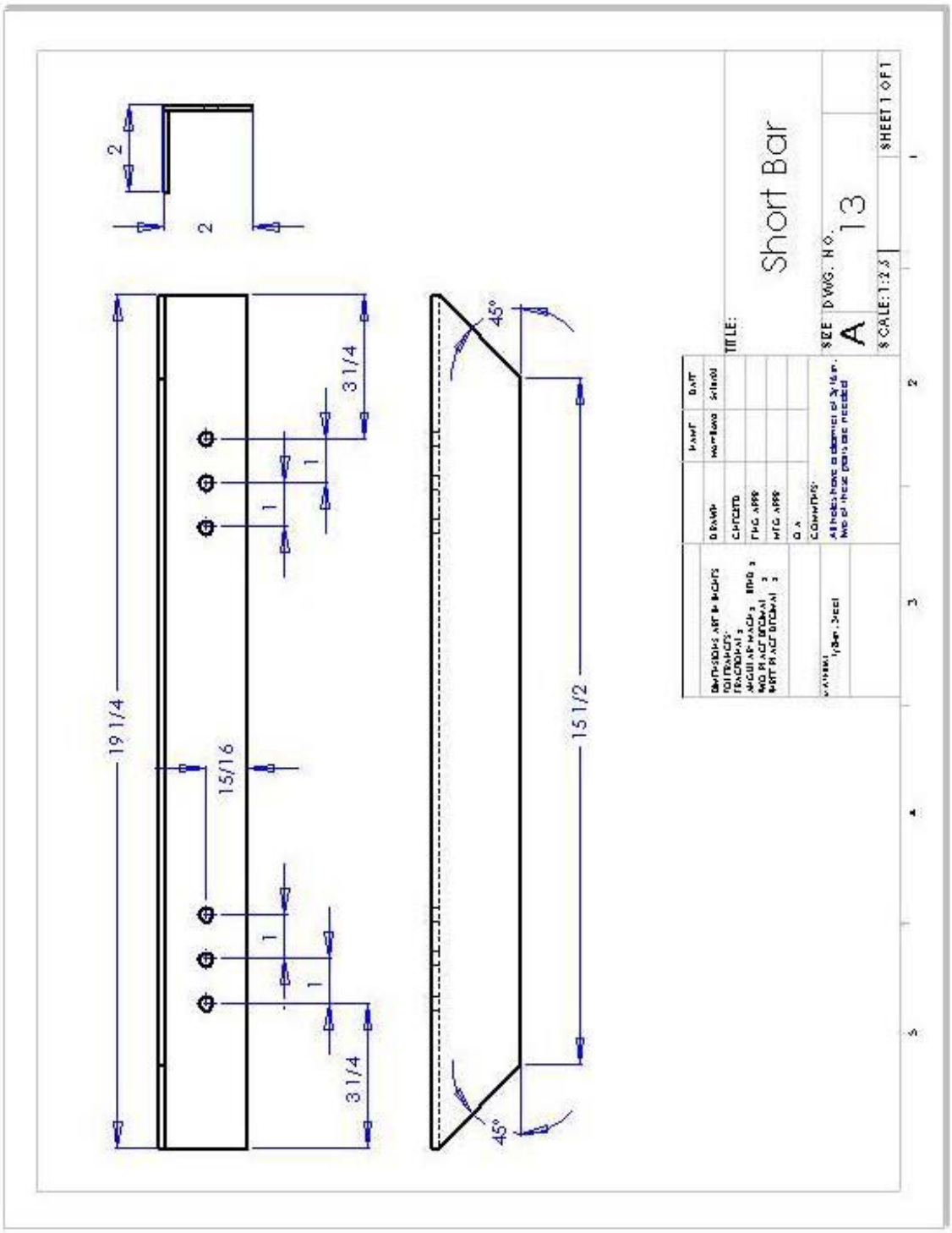
2
2
19 1/4
15/16
31/4
1
1
1
31/4
45°
15 1/2
45°
Short Bar
A
13

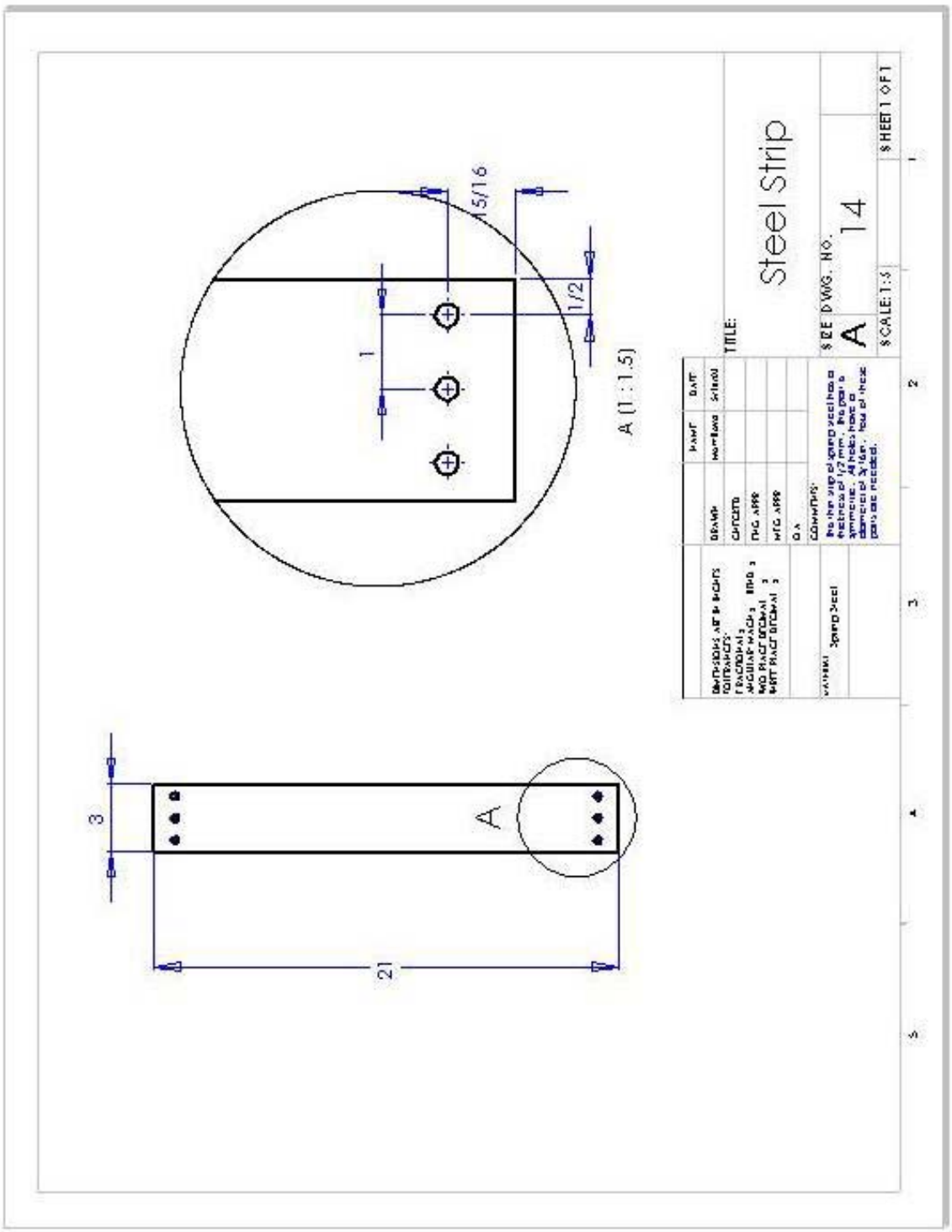
3
21
A
A (1 : 1.5)
15/16
1
1/2
TITLE:
Steel Strip
SIZE
A
DWG. NO.
14
SCALE: 1:3
SHEET 1 OF 1

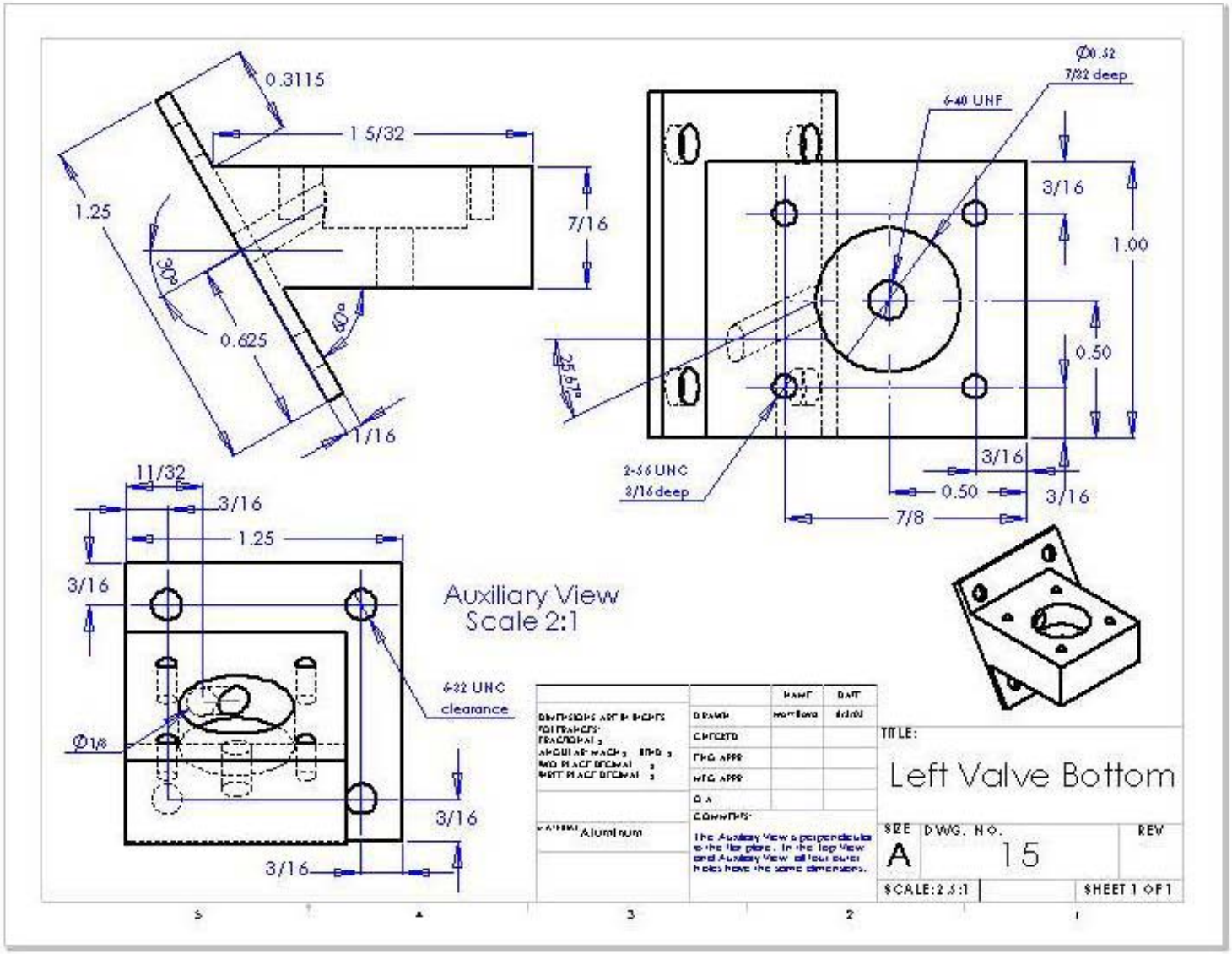
0.3115
1 5/32
1.25
7/16
30°
0.625
60°
1/16
Ø0.32
7/32 deep
6-40 UNF
3/16
1.00
0.50
25.67°
2-56 UNC
3/16 deep
3/16
0.50
3/16
7/8
11/32
3/16
1.25
3/16
6-32 UNC
clearance
Ø1/8
3/16
3/16
Auxiliary View
Scale 2:1
Aluminum
The Auxiliary View is perpendicular to the flat plate. In the Top View and Auxiliary View all four outer holes have the same dimensions.
TITLE:
Left Valve Bottom
SIZE
A
DWG. NO.
15
REV
SCALE: 2.5:1
SHEET 1 OF 1

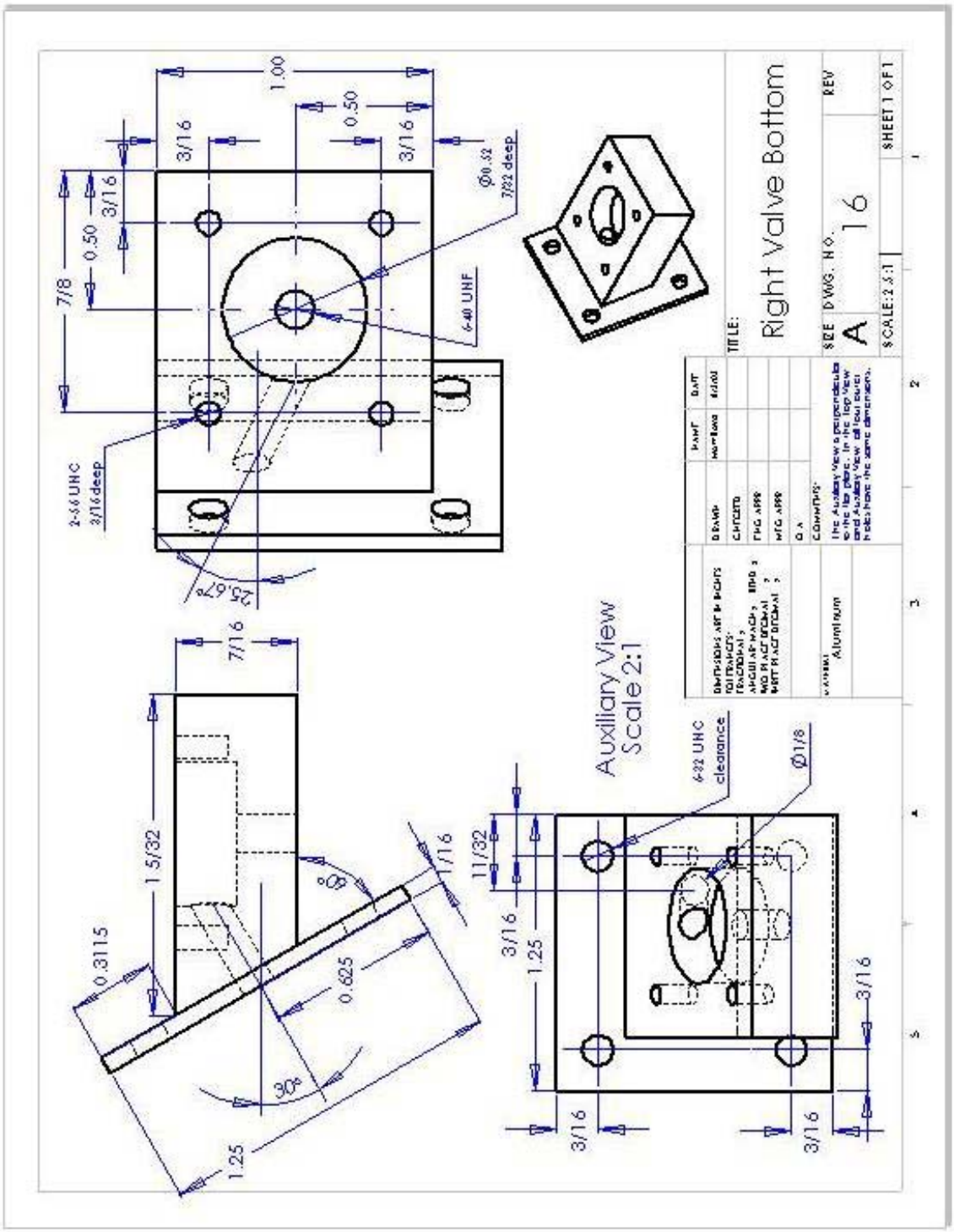
Right Valve Bottom
Auxiliary View
Scale 2:1
1.00
0.50
3/16
7/8
2-56 UNC
3/16 deep
6-40 UNF
Ø0.32
7/32 deep
25.67°
7/16
1.5/32
0.3115
0.625
30°
1.25
1/16
8°
11/32
1.25
6-32 UNC
clearance
Ø1/8
Aluminum
SIZE
A
DWG. NO.
16
REV
SCALE: 2:1
SHEET 1 OF 1

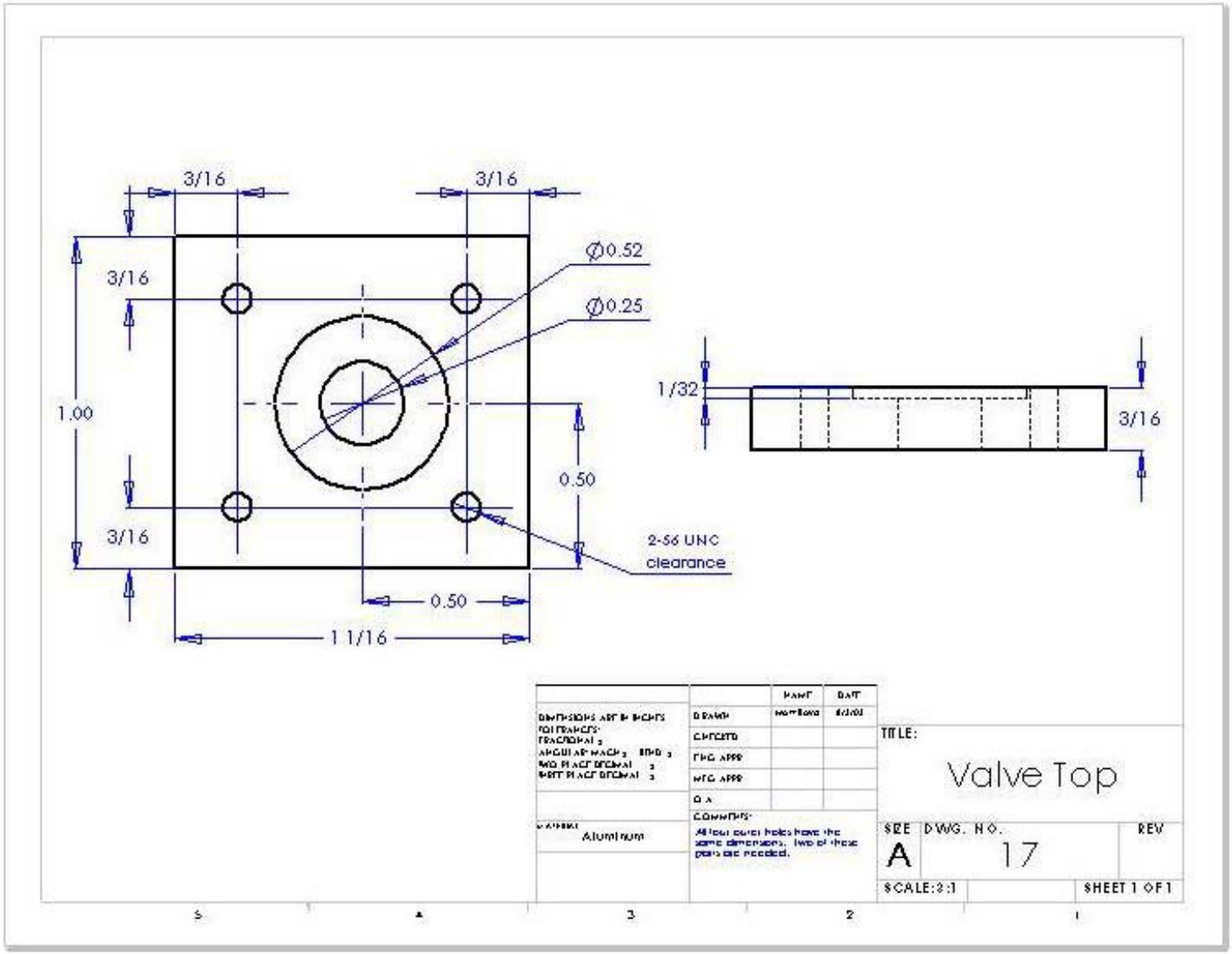
3/16
3/16
3/16
3/16
1.00
Ø0.52
Ø0.25
0.50
2-56 UNC
clearance
0.50
1 1/16
1/32
3/16
NAME
DATE
DRAWN
CHECKED
ENG APPR
MFG APPR
Q.A
COMMENTS:
All four outer holes have the same dimensions. Two of these parts are needed.
Aluminum
TITLE:
Valve Top
SIZE
A
DWG. NO.
17
REV
SCALE: 3:1
SHEET 1 OF 1

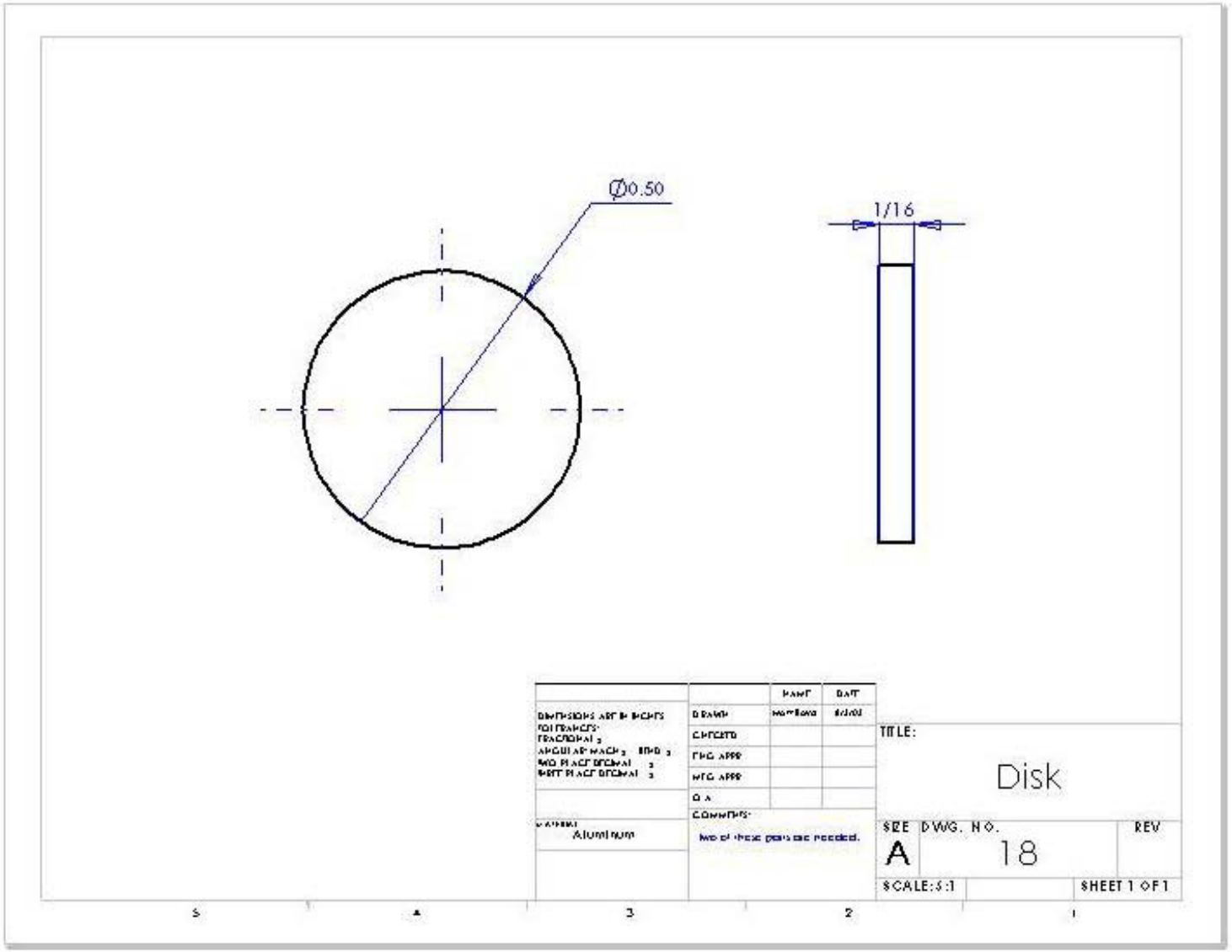
Ø0.50
1/16
NAME
DATE
DRAWN
CHECKED
ENG APPR
MFG APPR
Q.A
COMMENTS:
Aluminum
Two of these parts are needed.
TITLE:
Disk
SIZE
A
DWG. NO.
18
REV
SCALE: 5:1
SHEET 1 OF 1

BIBLIOGRAPHY

[1] Anderson, John D. Jr. Fundamentals of Aerodynamics Third Edition. McGraw-Hill Companies Inc.: New York, NY, 2001.

[2] Butcher, Bradley H., A Pneumatically-Powered Motion System for a High-Speed Scanner. Master's Thesis, Georgia Institute of Technology: Atlanta, GA, 2002.

[3] Fox, Robert W., McDonald, Alan T. Introduction to Fluid Mechanics Fifth Edition. John Wiley & Sons Inc.: New York, NY, 1998.

[4] Gere, James M., Timoshenko, Stephen P. Mechanics of Materials Fourth Edition. PWS Publishing Company: Boston, MA, 1997.

[5] Incropera, Frank P., DeWitt, David P. Fundamentals of Heat and Mass Transfer Fifth Edition. John Wiley & Sons Inc.: New York, NY, 2002.

[6] Ogata, Katsuhiko. Discrete-Time Control Systems Second Edition. Prentice-Hall Inc.: Upper Saddle River, NJ, 1995.

[7] Shapiro, Howard N., Moran, Michael J. Fundamentals of Engineering Thermodynamics 4th Ed. John Wiley & Sons Inc.: New York, NY, 2000.